Time-Series Momentum across the Capital Structure*

Thomas Gruenthaler †
Alberto Manconi ‡
Frans A. de Roon §
Zhaneta K. Tancheva ¶

August 21, 2026

Abstract

We develop and empirically test conditions for time-series momentum (TSM) and reversal across the capital structure. The conditions organize a unified pattern of predictability: equity returns exhibit TSM or reversal depending on firms' leverage and exposure to priced variance risk, corporate bonds reverse, and predictability spills over from equity to debt. The mechanism arises in a model where equity and debt are nonlinear claims on the firm's assets and variance risk is priced. Leverage generates reversal, variance-risk exposure generates continuation, and which force dominates depends on both together. Aggregating these firm-level forces into portfolios yields measures that predict momentum crashes.

Keywords: Momentum, credit risk, variance risk premium, stochastic variance

JEL: G12, G13

* We thank Vladimir Atanasov (discussant), Martijn Boons, Frank de Jong, Robert Dittmar, Joost Driessen, Bjørn Eraker, Lorenzo Garlappi, Amit Goyal, Joni Kokkonen (discussant), Juhani Linnainmaa, Lars Lochstoer, Philippe Mueller (discussant), Manuela Pedio (discussant), Joshua Rauh, Michael Roberts, Jacob Sagi, Nikolaus Schweizer, Bas Werker, Paul Whelan (discussant), Costas Xiouros, Guofu Zhou, participants at the EFA, St. Gallen Financial Economics Workshop, Frontiers of Factor Investing, Nova–BPI Asset Management, FMA European, Bristol Financial Markets, and NFN Young Scholars Nordic Finance conferences, as well as seminar participants at Tilburg University and BI Norwegian Business School for useful comments. We gratefully acknowledge an Inquire Europe Grant and the Quoniam Asset Management Innovation in Data-Driven Investing Prize. Any remaining errors are our own.

† Tilburg University, t.grunthaler@tilburguniversity.edu
‡ Bocconi University, alberto.manconi@unibocconi.it
§ Tilburg University, f.a.deroon@tilburguniversity.edu
¶ BI Norwegian Business School, zhaneta.k.tancheva@bi.no

1 Introduction

Equity and corporate debt are contingent claims on the same underlying assets (Merton, 1974), yet relatively little is known about their joint time-series return predictability at the firm level. For equities, the literature documents both time-series momentum (TSM) and reversal at different horizons (Goyal and Jegadeesh, 2018; Jegadeesh, 1990), but does not predict which firms' equity returns should continue and which should reverse. For corporate bonds and equity-to-bond predictability, the evidence is largely based on cross-sectional sorts (Dick-Nielsen, Feldhütter, Pedersen, and Stolborg, 2026; Gebhardt, Hvidkjaer, and Swaminathan, 2005; Jostova, Nikolova, Philipov, and Stahel, 2013). Taken together, this evidence leaves a central question unresolved: what determines the sign and transmission of time-series return predictability across a firm's capital structure?

We address this question by identifying two opposing channels of firm-level time-series return predictability: leverage, which generates reversal, and priced variance risk, which generates continuation. Each channel's strength depends on the other, so which force dominates is determined by the two together, rather than by either channel alone. We derive closed-form conditions characterizing this trade-off and show that a single mechanism unifies four predictions across corporate claims that we confirm empirically. First, equity predictability changes sign across firms: time-series momentum is concentrated among sufficiently levered firms with strong exposure to variance risk, while others reverse. Second, corporate bond returns strongly reverse. Third, continuation spills over from equity to debt: for highly levered, high-variance firms, past equity returns positively predict future bond returns. Finally, at the portfolio level, capital-structure asymmetries predict momentum crashes.

The key insight is that equity is a residual claim on firm assets and inherits a convex payoff (Merton, 1974).[1] A negative return shock therefore increases equity leverage and asset-risk exposure, raising expected returns and inducing reversal. At the same time, the shock raises equity's sensitivity to firm-level variance risk. When variance risk is negatively priced – meaning that assets that perform well when variance rises earn lower expected returns[2] – greater variance exposure lowers expected returns and instead induces continuation. Which force dominates depends on a nonlinear function of leverage and variance exposure rather than on either characteristic alone. The same logic extends across the capital structure. Because debt is concave in firm value, the variance channel reverses sign: greater variance exposure raises expected bond returns, generating own-bond reversal. Yet shared exposure to variance shocks moves realized equity returns and expected bond returns in the same direction, so past equity returns positively predict future bond returns even as bonds reverse with respect to their own past returns. At the portfolio level, higher leverage among past losers leaves the momentum strategy effectively short market rebounds, so the same asymmetry yields predictors of momentum crashes.

We formalize this mechanism with a deliberately tractable approach. We work in the tradition of Merton (1974), valuing equity as a call option on firm assets, and combine it with the top-down approach of Carr and Wu (2020). We use the Merton formula as an instantaneous valuation map rather than a literal description of the world, identifying at each date the asset value and variance input consistent

[1] Sagi and Seasholes (2007) and Garlappi and Yan (2011) develop related rational mechanisms in which nonlinear, option-like features of equity payoffs generate return continuation. Section 2 distinguishes our mechanism and predictions.

[2] Substantial evidence suggests that variance risk is negatively priced at the firm-asset level (Du, Elkamhi, and Ericsson, 2019; Zhang, Zhou, and Zhu, 2009), firm-equity level (Dickerson, Fournier, Jacobs, and Orlowski, 2026; Duarte, Jones, and Wang, 2024) and aggregate equity-market level (Bollerslev, Tauchen, and Zhou, 2009; Carr and Wu, 2009). Heston and Todorov (2025) document negative variance risk premiums across various asset classes.

with observed equity. We take this route, rather than specifying the dynamics of firm assets, because it yields an analytical condition determining which firms exhibit reversal and which continuation. A fully specified stochastic-volatility model reproduces the condition only numerically but yields nearly identical classifications.

To bring the framework to the data, we estimate the variance input following Bharath and Shumway (2008) and classify each firm-month by the sign of the condition. The condition links a current return innovation to the associated revision in expected returns and therefore does not itself imply horizon-specific predictions. Empirically, the innovation is not directly observable and must be proxied by past cumulative returns, creating a trade-off across formation horizons: short-horizon signals are closer to the underlying innovation but noisier, while longer-horizon signals are less sensitive to transitory noise but increasingly incorporate persistent differences in expected returns. Because persistent expected-return sorting can affect both condition-satisfying and condition-failing firms, we focus on the difference in time-series momentum returns between firms that satisfy and fail the condition, which more directly captures the differential continuation associated with the condition. We report this difference across formation horizons.[3]

We test the model in U.S. equity and corporate bond data. At every formation horizon, condition-satisfying firms earn higher time-series momentum returns than firms that fail the condition, with the difference peaking at 0.84% per month at the six-month formation horizon. Non-satisfying firms exhibit mild reversal at that horizon and significant reversal at shorter horizons. A distinctive implication emerges among low-leverage, low-variance firms, where the variance channel cannot dominate: returns reverse, as the leverage channel predicts. The difference between

[3] Section 4.2 discusses in detail how this comparison varies with the formation horizon.

the groups persists over longer holding periods and survives risk adjustment using the three- and five-factor models of Fama and French (1993, 2015).

A natural question is whether the condition merely repackages leverage, volatility, or credit quality, characteristics previously associated with *cross-sectional* momentum (Avramov, Chordia, Jostova, and Philipov, 2007; Zhang, 2006). It does not. In the time series, the model predicts a sign reversal at a model-implied boundary, rather than stronger continuation as leverage and variance rise. Within a leverage–volatility double sort, condition-satisfying firms continue to earn higher time-series momentum returns at every horizon, with the difference strongest at six months. In Fama and MacBeth (1973) regressions, the interaction between past returns and the condition remains significant after allowing past returns to interact separately with leverage, asset volatility, and credit rating. None of these interactions subsumes it. The condition's coefficient is essentially unchanged when past returns interact with leverage, asset volatility, and rating simultaneously. Return continuation is therefore not predicted by leverage, asset volatility, or credit quality in isolation, but by the combined effect of leverage and variance captured by the model-implied condition.

Turning to corporate bonds, the variance channel operates in reverse. Because debt is a concave claim on firm assets, higher variance exposure raises required bond returns rather than lowering them, predicting reversal rather than continuation in debt. The data bear this out. Consistent with the model's prediction, sorting bonds on their own past returns yields significantly negative time-series momentum across all horizons, at roughly -20 to -40 basis points per month.

Yet past equity returns can positively predict future bond returns. This equity-to-bond spillover is a central implication of the model: because equity and debt share the same underlying assets, equity continuation can carry over to bonds. We

show that spillover is positive when the variance channel dominates: a shock that raises variance lifts the realized equity return and raises the return investors require on the bond going forward. Since bond expected returns generally respond less to variance shocks, spillover requires more leverage than equity momentum does.

We confirm this pattern in the data. Sorting on the spillover condition, condition-satisfying firms earn nearly 1% per month at short horizons, compared with 0.15% for condition-failing firms. The effect is strongest at short horizons and fades as the lookback horizon lengthens. Two additional results help address potential concerns about this interpretation. First, spillover is not an illiquidity artifact. Sorting bonds by the Amihud (2002) measure and the fraction of zero-trading days, we find that the effect remains economically large and statistically significant among the most liquid bonds, where stale prices are least likely to generate predictability. Second, it concentrates where the model predicts, in speculative-grade issuers, where leverage and default risk matter most.

Although the model allows negative spillover among firms with weak exposure to variance risk, equity returns predict bond returns positively on average. This unconditional relation may reflect broader channels, such as market segmentation (Greenwood, Hanson, and Liao, 2018) and slow information diffusion (Gebhardt, Hvidkjaer, and Swaminathan, 2005). Our model contributes a distinct cross-sectional prediction, which the data strongly support: predictability is concentrated among the high-leverage, high-variance firms identified by the spillover condition.

Finally, the same firm-level exposures have a portfolio-level implication for cross-sectional momentum crashes. After a market downturn, losers become more levered and more option-like than winners, loading more heavily on aggregate asset and variance shocks. The winner-minus-loser portfolio therefore inherits a negative loading

on common shocks and is effectively short a market rebound. A large positive shock lifts losers more than winners, producing a sharp negative momentum return. This fragility intensifies with the fraction of firms satisfying the equity time-series momentum condition: a higher fraction indicates that the high-exposure state is widespread across the cross-section and signals more extreme aggregate winner–loser loadings, leaving the strategy exposed to common shocks. Crashes can thus arise from the asymmetry in winners' and losers' loadings alone, without fat tails or additional nonlinearities in realized returns.

The data are consistent with this mechanism. Defining a momentum crash as a bottom-5% winner-minus-loser return, we show that several model-implied variables predict crash episodes in sample, even after controlling for the aggregate crash predictors of Daniel and Moskowitz (2016), past market returns and market volatility. The fraction of firms satisfying the equity time-series momentum condition positively predicts crashes. Moving this fraction from the 5–15% band that prevails in normal times to the 25–40% levels reached in downturns raises the predicted crash probability from the unconditional 5% to roughly 15–20%. Decomposing the strategy's shock exposures, the predictability is concentrated in the loser leg's asymmetric exposure to asset and variance shocks, so the cross-sectional structure of risk exposures carries information about crash risk beyond aggregate market conditions.

Taken together, our results show that a single mechanism organizes firm-level return predictability across the capital structure. Specifically, priced variance risk interacting with the firm's capital structure yields conditions that identify continuation in condition-satisfying equities and reversal where the condition fails, account for reversal in corporate bonds, generate firm-level equity-to-bond return spillover, and imply a portfolio-level mechanism for momentum crashes.

2 Relation to the Literature

The paper contributes to several strands of literature. First, our main theoretical contribution is to rational theories of return continuation and reversal. Existing rational accounts generate continuation through time-varying expected returns or risk (Johnson, 2002; Liu and Zhang, 2008). Most closely related to our mechanism are theories that exploit the nonlinear nature of corporate claims. Sagi and Seasholes (2007) show that nonlinear exposure to firm characteristics can generate continuation, while Garlappi and Yan (2011) show that shareholders' recovery options in distressed firms make equity beta hump-shaped in default risk, so that near distress a price decline lowers expected returns and generates continuation among low-credit-quality firms. McQuade (2018) embeds priced stochastic volatility in a structural model of the firm and notes that, because distressed equity hedges variance risk, momentum profits should concentrate among low-rated firms. Momentum, however, remains a qualitative implication of his analysis of credit spreads and the distress anomaly rather than a formally characterized prediction.

We build on the common insight that nonlinear corporate claims can generate return continuation, but sharpen it in three ways. First, priced variance risk introduces a continuation channel that competes with leverage-induced reversal, yielding a closed-form condition that determines the sign of firm-level return predictability. Second, applying the same condition across corporate claims jointly predicts which firms' equities exhibit continuation or reversal, why corporate bonds reverse, and when past equity returns positively predict future bond returns. To the best of our knowledge, no prior theory derives this joint pattern of sign and transmission across the capital structure. Finally, aggregating the same firm-level exposures into

winner-minus-loser portfolios yields implications for momentum-crash risk.

Second, we contribute to the literature on time-series momentum. Moskowitz, Ooi, and Pedersen (2012) document time-series momentum across asset classes, while Huang, Li, Wang, and Zhou (2020) show that the unconditional asset-level evidence is statistically fragile. Goyal and Jegadeesh (2018) find sizable TSM in individual stocks. We complement the broader TSM literature by identifying a capital-structure mechanism for time-series predictability in corporate claims. The interaction between leverage and variance exposure determines whether equity exhibits continuation or reversal, linking TSM to observable firm characteristics and identifying where each should arise. This prediction echoes the *cross-sectional* momentum literature, where momentum is known to concentrate among firms with high leverage, low credit quality, and high volatility (Avramov, Chordia, Jostova, and Philipov, 2007; Zhang, 2006). We show that these characteristics also organize firm-level time-series momentum through the model-implied condition that combines them.

Third, we connect our mechanism to the literature on corporate-bond momentum and equity-to-bond predictability. Jostova, Nikolova, Philipov, and Stahel (2013) document cross-sectional momentum in corporate bonds, though it weakens under cleaner TRACE-based data (Dick-Nielsen, Feldhütter, Pedersen, and Stolborg, 2026). Gebhardt, Hvidkjaer, and Swaminathan (2005) show that past equity returns predict bond returns in the cross-section (see also Chordia, Goyal, Nozawa, Subrahmanyam, and Tong (2017) and Choi and Kim (2018)). Related work studies return transmission at more aggregate levels: Pitkäjärvi, Suominen, and Vaittinen (2020) document that past equity market returns are negative predictors of future bond market returns, while Keshavarz and Sirmans (2026) show that lagged corporate-

bond factor returns predict matched equity-factor returns. Dickerson, Fournier, Jeanneret, and Mueller (2025) instead explain the contemporaneous comovement of a firm's stock and bonds through common priced fundamentals in a structural credit-risk model. These papers establish important links between equity and bond returns, but do not characterize the firm-level time-series predictability across the two claims that we study. We make two contributions along this dimension. First, we show why corporate bonds should exhibit own-return reversal: because debt is concave in firm value, the variance channel that generates continuation in equity operates in the opposite direction for debt. Second, we derive a firm-level condition under which past equity returns positively predict the same firm's future bond returns. This prediction is distinct from the established cross-sectional spillover and ties equity-to-bond predictability to the same leverage and variance channels that govern equity continuation and bond reversal.

Fourth, we connect the same mechanism to the literature on momentum crashes. Daniel and Moskowitz (2016) show that crashes occur in panic states following market declines and are predictable from past market returns and volatility, while Barroso and Santa-Clara (2015) show that volatility scaling substantially reduces crash risk. We complement this aggregate-state perspective by showing that crash risk depends on asymmetries in common-shock exposures between momentum winners and losers. In particular, crash risk rises as losers become more exposed than winners to common asset and variance shocks, even under Gaussian shocks without fat tails or nonlinear return dynamics. Empirically, the corresponding model-implied exposure measures predict momentum crashes beyond the aggregate market conditions identified by Daniel and Moskowitz (2016). Our contribution is to identify a mechanism for momentum-crash risk and the exposure measures it implies, rather than to pro-

vide a quantitative account of realized crash magnitudes. Thus, the same firm-level leverage and variance channels that govern continuation, reversal, and equity-to-bond predictability also generate a portfolio-level source of momentum-crash risk.

Finally, we build on the structural credit-risk literature initiated by Merton (1974). In the standard Merton model, expected security returns are linear in expected asset growth, ruling out momentum when fundamentals are independently distributed. We show that this implication changes once variance is priced. Rather than fully specifying all underlying state-variable dynamics, we treat the variance input to Black–Scholes–Merton valuation as a priced state variable, following the top-down approach of Carr and Wu (2020) and building on structural models with time-varying variance at the equity-credit intersection (Chen, Collin-Dufresne, and Goldstein, 2009; Collin-Dufresne, Junge, and Trolle, 2024; Cremers, Driessen, and Maenhout, 2008; Dickerson, Fournier, Jeanneret, and Mueller, 2025). Our use of priced variance risk is closest to structural models with stochastic variance (Du, Elkamhi, and Ericsson, 2019; Zhang, Zhou, and Zhu, 2009), though we treat the input variance as a reduced-form pricing state summarizing risks not explicitly modeled in our framework. Because estimates of the price of variance risk in such specifications may partly absorb compensation for omitted risks, they provide a natural benchmark for its sign and magnitude in our setting. Treating variance as a priced state variable preserves closed-form expected-return expressions while yielding analytical conditions in observable firm characteristics. This links structural credit-risk models with stochastic variance to time-series return predictability: the same framework can generate both TSM and reversal across firms.

3 Model

3.1 General Framework

In the baseline Merton (1974) framework, equity is a contingent claim on firm assets. Return shocks change equity leverage and can therefore generate time-series reversal, but not continuation when expected asset returns are independently distributed.[4] Continuation requires an additional priced state variable that affects expected returns.

Rather than specifying a fully structural model of all underlying state variables, we follow Carr and Wu (2020) and adopt a top-down valuation approach. Their framework links option values directly to profit-and-loss attribution and provides a tractable representation of expected returns while preserving closed-form valuation expressions. This is attractive in our setting because it lets us introduce an additional priced state variable while retaining analytical tractability.

We value equity $E(t, A(t), F, V(t), T)$ as a call option on total assets $A(t)$ with variance $V(t)$, using the Black–Scholes–Merton formula. Each firm issues a single class of debt, a zero-coupon bond with face value F and maturity date T, such that

$$E = A\,\Phi\left(\frac{\log\left(\frac{A}{Fe^{-\tau r_f}}\right) + \frac{V}{2}\tau}{\sqrt{V\,\tau}}\right) - Fe^{-\tau r_f}\,\Phi\left(\frac{\log\left(\frac{A}{Fe^{-\tau r_f}}\right) - \frac{V}{2}\tau}{\sqrt{V\,\tau}}\right), \tag{1}$$

where we suppress the arguments of E, A, and V whenever they are obvious and define time-to-maturity $\tau = T - t$ and the risk-free rate r_f.

Two features of this setup are central. First, the Black–Scholes–Merton formula

[4] Expected log returns also depend mechanically on volatility through the Jensen term, so even the baseline Merton model can generate variation in expected log returns. Our object, however, is predictability in simple returns.

is used as a valuation map rather than as a literal description of the data-generating process: the framework does not require the model to be true, but exploits the fact that the variance input is a convenient summary statistic for the risks that affect equity value. This preserves closed-form pricing expressions and keeps the empirical implementation light. Second, $V(t)$ is the variance input to this map – the variance that reprices equity – and we treat it as a priced state variable rather than as an estimate of instantaneous asset variance. It is worth being precise about what V is. It is the number that, fed through the valuation map, is consistent with the observed equity value at each date. It is a reduced-form pricing state that summarizes the compensation-relevant risks bearing on equity, not a measurement of the physical variance of assets. Empirically, we estimate it with the iterative procedure of Bharath and Shumway (2008). The procedure has its lineage in the KMV distance-to-default tradition, which likewise uses the Merton map to recover unobserved firm-level quantities from observed equity.

The instantaneous change in equity value can be approximated by a second-order Taylor expansion:

$$dE = -E_\tau dt + E_A\, dA + E_V dV + \frac{1}{2}E_{AA}\,(dA)^2 + \frac{1}{2}E_{VV}\,(dV)^2 + E_{AV}\, dA\, dV, \qquad (2)$$

where E_τ, E_A, E_V, E_{AA}, E_{VV}, and E_{AV} denote partial derivatives of equity with respect to time-to-maturity τ, total assets A, and variance V. The expansion is accurate to second order and therefore introduces an approximation error that is negligible over the typical investment horizon (Carr and Wu, 2020).[5] The partial derivatives correspond to familiar option Greeks and summarize how equity responds

[5] We abstract from potential higher-order terms arising from jumps.

to asset shocks, input variance shocks, and their interaction.[6]

To characterize expected returns, we compare physical ($\mathbb{P}$) and risk-neutral ($\mathbb{Q}$) expectations of (2). This yields

$$\mathbb{E}_t^{\mathbb{P}}[dE] - \mathbb{E}_t^{\mathbb{Q}}[dE] = \Big[E_A A(\mu(t) - r_f(t)) + E_V(\mu_V^{\mathbb{P}}(t) - \mu_V^{\mathbb{Q}}(t))\Big]dt, \tag{3}$$

where $\mu(t)$ and $\mu_V(t)$ denote unspecified processes for the drifts of total assets and input variance. The equation is a general risk-premium decomposition, and holds for any diffusion dynamics of A and V.[7]

3.2 Specific Model: Stochastic Input Variance

The particular specifications of the dynamics of the state variables A and V determine which risk premia appear in (3) and how they are interpreted. While our approach is very flexible, we will focus on modeling the input variance directly. This approach is similar to the literature on pricing options on stock market variance (VIX).[8] Under the physical measure $\mathbb{P}$, the dynamics are given by:

$$\begin{aligned} \frac{dA}{A} &= \mu\, dt + \sigma_A\, dW^{A,\mathbb{P}} \\ dV &= \kappa(\theta - V)\, dt + \sigma_V \sqrt{V}\, dW^{V,\mathbb{P}}, \end{aligned} \tag{4}$$

where μ is the expected return on the firm's assets, κ the mean-reversion speed, and θ the mean-reversion level of the input variance. σ_A and σ_V are volatility parameters.

[6] The sensitivities with respect to V have to be expressed in terms of variance, not volatility.

[7] Girsanov's theorem implies that the change of measure shifts only the drifts of A and V. The E_{AA}, E_{VV}, and E_{AV} terms in (3) therefore vanish.

[8] For instance, Mencía and Sentana (2013) assume an exogenous process for variance when pricing VIX options instead of deriving the VIX from the underlying stock return dynamics, and specify both a physical process, governing the actual evolution of variance, and a risk-neutral process, used for pricing, connected through a market price of variance risk.

The Brownian shocks are correlated via ρ. Under the risk-neutral measure $\mathbb{Q}$, the dynamics evolve as:

$$\begin{aligned} \frac{dA}{A} &= r_f\, dt + \sigma_A\, dW^{A,\mathbb{Q}} \\ dV &= \kappa^{\mathbb{Q}}(\theta^{\mathbb{Q}} - V)\, dt + \sigma_V \sqrt{V}\, dW^{V,\mathbb{Q}}, \end{aligned} \tag{5}$$

where $\kappa^{\mathbb{Q}} = \kappa + \lambda_V$ and $\theta^{\mathbb{Q}} = \frac{\kappa\theta}{\kappa+\lambda_V}$. The parameter λ_V is the price of risk for the input variance. We impose the same correlation ρ under the risk-neutral measure.

We treat λ_V as common across firms. It prices the systematic component of variance risk, so cross-firm heterogeneity enters through firms' exposures to it, not through firm-specific prices of risk. A common price is consistent with the strong factor structure in firm-level volatility (Herskovic, Kelly, Lustig, and Van Nieuwerburgh, 2016), and we calibrate λ_V from the credit-spread and CDS literature that identifies this compensation directly (Du, Elkamhi, and Ericsson, 2019; Zhang, Zhou, and Zhu, 2009).[9]

The setup of the model differs from the standard approach in which assets have a time-varying variance (Collin-Dufresne, Junge, and Trolle, 2024; Du, Elkamhi, and Ericsson, 2019; Zhang, Zhou, and Zhu, 2009, among others). In our setup V is not the instantaneous asset variance (the instantaneous variance rate of asset returns is σ_A^2). It is the priced variance input to the valuation map, whose dynamics we model as a stochastic variance process. We adopt the stochastic-variance interpretation throughout. Section 3.2.3 shows that the momentum condition is robust to a fully structural stochastic-variance model that yields nearly identical firm classifications.

[9] Note that we calibrate $\lambda_V = -1.75$ to the median estimate in Du, Elkamhi, and Ericsson (2019). The empirical tests, however, use only the sign structure of the momentum condition and Table IA.1 shows that the resulting return spread is robust to values of λ_V between -3 and -0.5.

3.2.1 A Condition for Time-Series Momentum

Inserting the model dynamics into equation (3), the expression simplifies to:

$$\mathbb{E}_t^{\mathbb{P}}[dE] - \mathbb{E}_t^{\mathbb{Q}}[dE] = \left(E_A A(\mu - r_f) + E_V V \lambda_V\right) dt, \tag{6}$$

where $\mathbb{E}_t$ is the conditional expectation at time t. Hence, the expected change in equity consists of a leverage premium term $E_A A(\mu - r_f)$ and a variance premium term $E_V V \lambda_V$. Substituting $\mathbb{E}_t^{\mathbb{Q}}[dE] = r_f E\, dt$ and dividing (6) by E, we get the expected simple equity return:

$$g(t) = \frac{\mathbb{E}_t^{\mathbb{P}}[dE]/E}{dt} = r_f + \eta^A(\mu - r_f) + \eta^V \lambda_V, \tag{7}$$

where $\eta^A = E_A \frac{A}{E}$ and $\eta^V = E_V \frac{V}{E}$ denote the elasticities of the value of equity with respect to the value of assets and the input variance, respectively. The realized return is given by

$$r(t) = \frac{1}{E}\Big(E_A \sigma_A A\, dW^A + E_V \sigma_V \sqrt{V}\, dW^V + O(dt)\Big). \tag{8}$$

Equation (7) is the building block of the model. The key insight is that expected returns evolve through two competing channels. The first is a leverage channel. Following poor performance, equity becomes a smaller fraction of firm value, increasing leverage and exposure to asset risk. This channel tends to raise future expected returns and therefore generates return reversal. The second is a variance channel. Poor performance also increases the option-like component of equity and therefore its exposure to variance risk. Consistent with empirical evidence that variance risk is negatively priced, this channel lowers future expected returns and generates re-

turn continuation. Momentum emerges whenever the variance channel dominates the leverage channel. As we show below, the joint effect of the leverage and variance channels yields a closed-form condition for equity time-series momentum.

We characterize the sign of time-series predictability through the conditional covariance between innovations in expected returns and realized returns, following Sagi and Seasholes (2007). A positive covariance implies continuation, while a negative covariance implies reversal. This perspective links realized returns to revisions in expected returns, with the sign determining continuation or reversal.

Definition 1 (Equity Time-Series Momentum Condition)**.** *A firm's equity exhibits time-series momentum (TSM) at time t if and only if*

$$\mathrm{Cov}_t(dg(t), r(t)) > 0. \tag{9}$$

Conversely, $\mathrm{Cov}_t(dg(t), r(t)) < 0$ implies time-series reversal. For $s < t$ with $t = s + dt$, an Itô expansion implies $g(t) = g(s) + dg(s) + O(dt)$. Let $\mathcal{F}_s$ denote the information available at time s. Conditioning on $\mathcal{F}_s$, the term $g(s)$ is known, so it does not covary with the realized return $r(t)$ over $[s, t]$. Hence

$$\mathrm{Cov}_s(r(t),\, g(t)) = \mathrm{Cov}_s(r(t),\, dg(s)) + o(dt),$$

where $r(t)$ and $dg(s)$ are both driven by the Brownian increments over $[s, t]$. Consequently, condition (9) is equivalent, to first order in dt, to $\mathrm{Cov}_s(r(t), g(t)) > 0$: the momentum condition can be stated equivalently in terms of the level of g at the end of the period rather than its instantaneous increment.

In our model, the change in expected returns is given by

$$dg = g_A \, \sigma_A \, A \, dW^A + g_V \, \sigma_V \, \sqrt{V} \, dW^V + O(dt), \tag{10}$$

where

$$g_A = \frac{\partial \eta^A}{\partial A}(\mu - r_f) + \frac{\partial \eta^V}{\partial A}\lambda_V, \qquad g_V = \frac{\partial \eta^A}{\partial V}(\mu - r_f) + \frac{\partial \eta^V}{\partial V}\lambda_V. \tag{11}$$

The term $O(dt)$ collects all drift terms. At order dt, only the martingale components contribute to the covariance. Therefore,

$$\frac{\mathrm{Cov}_t(dg, r)}{dt} = \frac{1}{E}\left(g_A E_A \sigma_A^2 A^2 + g_V E_V \sigma_V^2 V + \rho \, \sigma_A \sigma_V A \sqrt{V} \, (g_A E_V + g_V E_A)\right), \tag{12}$$

because $(dt)^2 = 0$, $dt \, dW = 0$, $(dW)^2 = dt$, and $dW^A dW^V = \rho \, dt$.

Equation (12) yields a closed-form expression for the sign of time-series predictability. Equity exhibits TSM when the expression is positive and reversal when it is negative. The condition decomposes the own-return predictability into three components: an asset term, a variance term, and a cross term. Appendix A derives analytical expressions for the relevant partial derivatives. Three of the four derivatives are unambiguously negative, while $\frac{\partial \eta^V}{\partial V}$ can change sign depending on the firm's leverage and variance state. It is generally negative for very high variance states but more likely to become positive for low-levered firms ($A \gg F$).

3.2.2 Economic Interpretation

Figure 1 illustrates how the sign of equation (12) varies across leverage and variance states. Both dimensions play a central role in determining whether a firm exhibits

TSM or reversal. Low-risk firms, characterized by low leverage and low input variance, are dominated by the leverage channel and therefore tend to exhibit reversal. In contrast, firms with high leverage and/or high input variance are dominated by the variance channel and therefore exhibit momentum. Put differently, momentum arises precisely among firms whose equity values are most sensitive to variance risk. Note that high leverage strengthens both channels, but in sufficiently levered, high-variance firms the variance-risk channel dominates, so momentum reflects the joint effect of leverage and variance rather than high leverage alone.

This prediction echoes the existing *cross-sectional* momentum literature. Prior studies show that momentum profits are strongest among firms with high leverage, low credit quality, and high volatility or distress risk. For example, Avramov, Chordia, Jostova, and Philipov (2007) document strong momentum among low-rated firms. Our framework predicts an analogous concentration of time-series momentum among firms for which the variance channel dominates the leverage channel.

3.2.3 Comparison with a Structural Stochastic-Variance Model

We treat equity as an option on firm assets and allow the option's volatility input to evolve as a priced stochastic state variable. Within the model, this input serves as a summary statistic for the time-varying risk compensation investors require. Modeling it as a mean-reverting variance process and pricing its risk through λ_V allows us to derive expected returns in closed form while treating V as a reduced-form summary of underlying risks.

A fully structural stochastic-variance model would give the underlying risk a specific economic interpretation, but at the cost of the closed-form sign boundary and without materially changing our results. To see this, consider the stochastic

asset-variance model of Du, Elkamhi, and Ericsson (2019), in which asset variance follows the square-root process of Heston (1993). The momentum condition is based on the covariance between changes in expected and realized returns:

$$\frac{\mathrm{Cov}_t^{SV}(dg, r)}{dt} = \frac{1}{E}\left(g_A^{SV} E_A V A^2 + g_V^{SV} E_V \sigma_V^2 V + \rho\, \sigma_V\, A\, V\, (g_A^{SV} E_V + g_V^{SV} E_A)\right), \tag{13}$$

where g_A^{SV} and g_V^{SV} denote the expected-return sensitivities. The expression is nearly identical to (12) with two differences: (i) σ_A^2 is replaced by V in the first and third terms, and (ii) prices and sensitivities are obtained from the characteristic function and are available only in semi-closed form, requiring the evaluation of a one-dimensional numerical integral. Despite these differences, the sign of the condition – and hence the classification of firms into momentum and reversal regions – is governed by the same three competing terms in both models. Figure IA.1 illustrates the equity time-series momentum condition implied by the stochastic asset-variance model and its overlap with the condition from our baseline model. The classifications agree for 92.5% of firms, while the disagreements are concentrated precisely around the zero boundary, where the momentum condition is economically indifferent.

3.2.4 Simulation Evidence

We next examine whether the model generates economically meaningful time-series momentum and whether the condition in Definition 1 successfully identifies firms that exhibit return continuation.

We simulate 20 independent panels of 5,000 firms. All firms begin with identical asset values, $A = 100$, while heterogeneity arises through differences in leverage and the initial level of the input variance. Specifically, the face value of debt, F, is drawn

uniformly from the interval $[10, 99]$, and the initial variance V is drawn uniformly from the interval $[0.03, 0.16]$. The price of asset risk is set to $\mu - r_f = 4\%$ and the price of variance risk to $\lambda_V = -1.75$. Debt maturity is fixed at $\tau = 1$ year, and the parameters that determine equation (12) are $\sigma_A = 0.09$, $\sigma_V = 0.40$, and $\rho = -0.15$, chosen to match the median estimates in Du, Elkamhi, and Ericsson (2019). To simulate the input variance dynamics, we set $\kappa = 2.50$ and $\theta = 0.07$.

Table 1 reports firm-level time-series momentum profits for lookback horizons $h \in \{1, 2, 3, 6, 12\}$ months. Following Goyal and Jegadeesh (2018), we construct a time-series momentum signal from the firm's cumulative excess return over the previous h months. Firms are held long when their past excess return is positive and short when it is negative, and returns are measured over the subsequent month. Columns partition firms according to the average value of the model-implied covariance $\mathrm{Cov}_t(dg, r)$ based on equation (12). Firms with positive covariance appear in the $\mathrm{Cov}_t > 0$ column and firms with negative covariance in the $\mathrm{Cov}_t < 0$ column; the former are the firms satisfying the time-series momentum condition in equation (9).

The momentum condition successfully separates firms with return continuation from those with return reversal, with the sharpest distinction at short horizons. The spread between the two groups is positive at every horizon, but the contrast is most pronounced at one month: firms in the $\mathrm{Cov}_t < 0$ column exhibit substantial reversal (-0.03%), whereas firms in the $\mathrm{Cov}_t > 0$ column display continuation (0.05%). This short-horizon reversal among firms with $\mathrm{Cov}_t < 0$ is precisely what the leverage channel predicts in the low-risk region of the state space. The reversal side of the boundary is therefore a direct prediction of the model that the simulation confirms, rather than a residual outcome.

As the horizon lengthens, a common momentum component emerges in both

groups, narrowing the spread even as profits rise. This reflects expected-return sorting: longer lookback windows increasingly sort firms on persistent differences in expected returns rather than on the shock continuation governed by the condition.[10]

Overall, the simulation results support the model's central mechanism. The condition in equation (12) identifies the firms for which the variance channel dominates, and it does so most clearly where the leverage channel would otherwise generate reversal. Simulated momentum profits are an order of magnitude below their empirical counterparts in Section 4.2, but this gap is not surprising given the model calibration. Because all firms share common parameters, the simulation compresses the cross-sectional dispersion in expected-return innovations that generates momentum profits. We therefore interpret Table 1 as evidence on signs and orderings – which firms continue, which reverse, and where the separation is strongest – rather than on magnitudes.

3.3 Momentum in Corporate Bonds

The previous subsection establishes that equity momentum arises when the variance channel dominates the leverage channel. We now ask whether the same mechanism generates momentum in corporate bonds. A firm's total assets are the sum of equity and debt, so we price debt via the identity $D = A - E$. Writing the bond's elasticities as $\zeta^A = D_A A/D$ and $\zeta^V = D_V V/D$, expected bond returns follow directly from those of equity,

$$g^D = \frac{\mathbb{E}_t^{\mathbb{P}}[dD]/D}{dt} = r_f + \zeta^A(\mu - r_f) + \zeta^V \lambda_V, \tag{14}$$

with $D_A = 1 - E_A = \Phi(-d_1)$ the bond delta and $D_V = -E_V$. Let $r^D(t)$ denote the realized bond return. The bond analogue of Definition 1 is given below.

[10] Section 4.2 discusses this more thoroughly.

Definition 2 (Bond Time-Series Momentum Condition)**.** *A firm's bond exhibits time-series momentum (TSM) at time t if and only if*

$$\mathrm{Cov}_t(dg^D(t), r^D(t)) > 0. \tag{15}$$

Conversely, $\mathrm{Cov}_t(dg^D(t), r^D(t)) < 0$ implies time-series reversal. The convention is the same as for equity. A positive covariance between innovations in expected bond returns and realized bond returns means continuation, a negative one reversal. Written out, the covariance in condition (15) is

$$\frac{\mathrm{Cov}_t(dg^D(t), r^D(t))}{dt} = \frac{1}{D}\Big[g^D_A D_A \sigma_A^2 A^2 + g^D_V D_V \sigma_V^2 V + \rho\, \sigma_A \sigma_V A\sqrt{V}(g^D_A D_V + g^D_V D_A)\Big], \tag{16}$$

where $g^D_A = \partial g^D/\partial A$ and $g^D_V = \partial g^D/\partial V$.

Substituting the debt identity into the elasticities,

$$\zeta^A = \frac{A}{D} - \frac{E}{D}\eta^A, \qquad \zeta^V = -\frac{E}{D}\eta^V, \tag{17}$$

exposes the asymmetry. The variance elasticity of debt is exactly the negative of equity's, rescaled by E/D. Since $\eta^V > 0$, it follows that $\zeta^V < 0$.

This sign reversal causes the variance channel to operate in opposite directions for equity and debt. For equity, a negative asset shock increases exposure to negatively priced variance risk, lowering expected returns and generating continuation. For debt, variance exposure has the opposite sign. The variance channel's contribution to expected bond returns, $\zeta^V \lambda_V$, is positive because $\lambda_V < 0$, so higher variance raises required bond returns. Realized bond returns, however, fall when variance rises, since $D_V = -E_V < 0$. Expected and realized bond returns therefore move in

opposite directions through the variance channel. Thus, the same channel that can generate positive momentum in equity produces reversal in debt.

The leverage channel is the only force that can generate bond TSM, since $g_A^D D_A \sigma_A^2 A^2 > 0$, but it is structurally weak. As a firm approaches risk-freeness, $D_A \to 0$, so changes in asset value have little effect on bond prices, while g_A^D is governed by the curvature of debt's concave payoff ($D_{AA} = -E_{AA} < 0$). The leverage channel can dominate only close to distress, where D_A approaches one, and at very short maturities, where the asset shock mechanically dominates a nearly linear payoff. This requires a near-default firm with only a few months remaining to maturity, a region absent from our sample of bonds with at least one year to maturity. Outside this narrow region, the variance channel dominates, and the model predicts time-series reversal in U.S. corporate bond returns.

3.4 Equity-to-Bond Spillover

The same channel that generates reversal in a bond's own returns also creates predictability across the capital structure. Because equity and debt are claims on the same assets, shocks that change realized equity returns can also affect expected bond returns, making *past equity returns* informative about *future bond returns*. The sign of this spillover can vary across firms. To characterize it, we examine the covariance between innovations in expected bond returns dg^D and realized equity returns r:

$$\mathcal{S}_t = \frac{\mathrm{Cov}_t(dg^D, r)}{dt} = \frac{1}{E}\Big[g_A^D E_A \sigma_A^2 A^2 + g_V^D E_V \sigma_V^2 V + \rho\, \sigma_A \sigma_V A \sqrt{V}\,(g_A^D E_V + g_V^D E_A)\Big]. \tag{18}$$

Definition 3 (Equity-to-Bond Spillover Condition)**.** *Past equity returns positively predict future bond returns if and only if*

$$\mathcal{S}_t = \mathrm{Cov}_t(dg^D, r)/dt > 0. \tag{19}$$

When $\mathcal{S}_t > 0$, past equity returns positively predict future bond returns, even as the bond's own past return predicts reversal. Equation (18) highlights the distinction between own-bond predictability and equity-to-bond spillover. Bond momentum requires realized and expected *bond* returns to move together, whereas spillover requires only that realized *equity* returns carry information about future bond returns. The two conditions differ because equity and debt load differently on asset and variance shocks. The model can therefore simultaneously generate bond reversal and positive equity-to-bond spillover, linking both forms of predictability to the same underlying mechanism.

Decomposing $\mathcal{S}_t$ into asset, variance, and cross components clarifies the driving forces:

$$\mathcal{S}_t = \underbrace{g_A^D E_A \sigma_A^2 A^2/E}_{\text{asset}} + \underbrace{g_V^D E_V \sigma_V^2 V/E}_{\text{variance}} + \underbrace{\rho\, \sigma_A \sigma_V A\sqrt{V}\,(g_A^D E_V + g_V^D E_A)/E}_{\text{cross}}.$$

The variance term is the engine of the spillover. A variance innovation raises the realized equity return, because equity is long variance ($E_V > 0$), and raises the expected bond return, because the variance channel runs in reverse for debt ($g_V^D > 0$). The two move together, so a past equity return carries information about where the bond return is heading. This is the same variance-risk mechanism that generates

equity momentum.[11] The cross term is negative under $\rho < 0$, since the bracket $g_A^D E_V + g_V^D E_A$ is positive. The asset term is small throughout. Positive spillover therefore emerges when the variance contribution dominates the opposing cross term.

Three testable implications follow. First, equity-to-bond time-series spillover should arise when the spillover covariance, $\mathcal{S}_t = \mathrm{Cov}_t(dg^D, r)/dt$, is positive. Second, spillover should be concentrated in highly levered firms with high variance. The variance component strengthens with leverage and with E_V, both of which vanish for safe firms whose bonds are close to risk-free. Firms exhibiting spillover should therefore lie largely within the set satisfying the equity time-series momentum condition, since in both cases the variance channel dominates. Third, spillover can coexist with own-bond reversal, because $\mathrm{Cov}_t(dg^D, r)$ and $\mathrm{Cov}_t(dg^D, r^D)$ have different signs over part of the state space.

Figure 2 plots the sign of $\mathcal{S}_t$ as a function of leverage and the input variance in the simulated model. The green region denotes $\mathcal{S}_t > 0$, corresponding to positive spillover, while the red region denotes $\mathcal{S}_t < 0$. Positive spillover is concentrated among firms with both high leverage and high variance: leverage increases debt's sensitivity to changes in expected returns, while higher variance strengthens the positive variance component. By contrast, safe firms exhibit little spillover, since their debt is close to risk-free and past equity returns contain little information about future bond returns.

[11] Numerical evaluation confirms that $g_V^D > 0$ and $g_A^D E_V + g_V^D E_A > 0$ throughout the relevant region of leverage and the input variance.

4 Empirical Evidence

This section tests the main predictions of the model. We begin by testing the mechanism in U.S. equities, examining whether the model-implied covariance condition identifies both sides of the boundary: firms that exhibit time-series momentum and firms whose returns reverse. We then turn to corporate bonds and one of the model's most distinctive predictions: equity-to-bond momentum spillover. The theory implies that the same variance-risk mechanism that generates equity momentum also makes past equity returns predict future bond returns, even though bonds themselves exhibit reversal.

4.1 Data

We obtain monthly returns for common stocks (share codes 10 and 11) listed on the NYSE, Amex, and NASDAQ from CRSP over 1966–2024. To attenuate the influence of penny stocks and microcaps, we exclude stocks below the NYSE tenth-percentile market-capitalization breakpoint (Fama and French, 2008). We retain firm-months for which all required inputs are non-missing, so the estimation sample is the intersection of the model inputs, CRSP, and the risk-free series.

Estimating the variance input. To construct an empirical counterpart to the momentum condition in equation (12), we follow Bharath and Shumway (2008). The procedure uses equity volatility $\sigma_E(t)$ to get an initial estimate of the input volatility, $\sqrt{V(t)} = \sigma_E(t)\,\frac{E}{E+F}$, where F captures the face value of debt, measured as short-term debt plus one-half of long-term debt. This initial volatility estimate is then used to infer the market value of assets $A(t)$ from the pricing equation (1). This procedure produces implied time series of asset values and volatilities over

the preceding year. From the implied asset values, we compute asset returns and update the estimates of $\sqrt{V(t)}$. These updated volatility estimates are then fed back into the pricing equation to re-estimate $A(t)$, and the procedure is repeated until convergence. When evaluating the condition in equation (12) at date t, we use the estimate of $V(t-1)$ when forming portfolios at t. This procedure recovers $V(t)$ rather than σ_A because it backs out whatever volatility parameter, plugged into the pricing equation (1), reproduces the observed equity value. That is precisely how $V(t)$ is defined in the model. The procedure itself relies on trailing equity returns, so the resulting measure is backward-looking, while $V(t)$ in the model is a forward-looking priced variance input that summarizes omitted variance-related risks. Hence, we assume that the recovered variance state reflects firms' exposure to priced variance risk. Specifically, we treat the Bharath and Shumway (2008) estimate as an empirical proxy for $V(t)$, rather than as the theoretical state variable itself, and use it to rank firms along this dimension. Following Bharath and Shumway (2008), we set τ equal to one year.[12]

Parameters. Consistent with our model simulations, we fix the following parameters when evaluating the momentum condition. We set σ_A, the constant volatility of the physical asset process, equal to 0.09, the asset risk premium $\mu - r_f$ to 4%, the volatility of the variance process to $\sigma_V = 0.40$, the correlation between asset and input-variance shocks to $\rho = -0.15$, and the price of input variance risk to $\lambda_V = -1.75$. The parameters reflect the median estimates reported in Du, Elkamhi, and Ericsson (2019). Although Du, Elkamhi, and Ericsson (2019) estimate λ_V in a model in which V is the instantaneous variance of asset returns, their estimate remains informative for our calibration. Structural estimates of variance-risk prices

[12] The results are robust to using longer debt maturities.

are model dependent: when additional risks such as jumps are introduced, estimated market prices of risk adjust, because parameters in the more parsimonious specification absorb compensation for the omitted risks.[13] Our V is defined as a reduced-form state variable that summarizes such omitted risks, so estimates that absorb compensation for them provide a natural benchmark for λ_V. We therefore use these estimates to discipline the sign and magnitude of λ_V in our calibration.

Table 2 reports summary statistics. Panel A pools all firm-months while Panels B and C condition on the sign of the estimated $\widehat{\mathrm{Cov}}_t(dg, r)$ in the given month. The autocorrelation is a firm-level statistic: for each firm with at least 24 monthly observations we estimate the AR(1) coefficient of the covariance and assign the firm to Panel B or C by the sign of its mean covariance (this firm-level assignment applies only to the AR(1) row; all other rows classify firm-months month by month). Firms satisfying the equity momentum condition have roughly twice the leverage and input variance of firms that do not. The covariance is also persistent, with firm-level AR(1) coefficients averaging around 0.4 across panels, indicating that the model-implied classification is stable over time rather than driven by transient noise.

Figure 3 plots the fraction of firms that satisfy the equity time-series momentum condition over the period 1966–2024. On average about 12% of firm-months meet the condition, but the fraction varies substantially over time and moves with periods of market stress. After rising through the early 1970s, it peaks near 24% during the 1973–75 downturn and then settles into a 5–15% band through the 1980s and 1990s, with smaller upticks around the 1987 crash and the early-1990s recession. The fraction climbs again to roughly 24% during the 2000–01 dot-com bust and reaches its sample maximum of nearly 40% in 2009, at the trough of the financial crisis.

[13] See, for instance, the estimates in Zhang, Zhou, and Zhu (2009) across different models.

It remains elevated thereafter, spiking to about 28% around the 2020–21 pandemic period before easing toward 10% at the end of the sample. The condition is thus most prevalent precisely when leverage and volatility are high market-wide.

4.2 Time-Series Momentum in U.S. Equities

4.2.1 Implementation

As a first empirical test of our theory, we examine return predictability in equities at the firm level. Following Goyal and Jegadeesh (2018), a firm i is assigned a long position when its own past excess return $r^e_{i,t-h:t}$ (cumulated over months $t-h$ through t, at lookback horizons $h \in \{1, 2, 3, 6, 12\}$) is positive and a short position when it is negative, and we measure the return over the subsequent month $r_{i,t+1}$. Consistent with the time-series convention of Goyal and Jegadeesh (2018), the signal includes the most recent month and no month is skipped.

Before presenting the results, we clarify how the signal maps into the model. The expected return on the time-series momentum strategy is $\mathbb{E}_t\big[\text{sign}(r^e_{i,t-h:t})\, r_{i,t+1}\big]$. Because the sorting signal is known at t and $\mathbb{E}_t[r_{i,t+1}] = g_i(t)$, this is equivalently a statement about expected returns. The condition in equation (12), however, governs innovations in g_i rather than its level. Decomposing the expected return gives

$$\mathbb{E}\big[\text{sign}(r^e_{i,t-h:t})\, g_i(t-h)\big] + \mathbb{E}\big[\text{sign}(r^e_{i,t-h:t})\big(g_i(t) - g_i(t-h)\big)\big]\,. \tag{20}$$

The first term reflects sorting on persistent differences in expected-return levels. As the lookback horizon lengthens, cumulative returns increasingly sort firms on these level differences rather than on the recent return innovations governed by our condition. Importantly, this component would be present even if the condition were zero

for every firm and therefore does not arise from the local continuation mechanism captured by the condition. The second term represents revisions in expected returns over the formation window. Definition 1 governs the local component of these revisions associated with contemporaneous return innovations through $\mathrm{Cov}_t(dg, r)$, so its effect is most directly reflected at short horizons, when the sorting signal places greater weight on shocks. Because persistent expected-return sorting can affect both condition-satisfying and condition-failing firms, we also report *Diff*, the difference in time-series momentum returns between firms that satisfy and fail the condition, which better captures the differential continuation associated with the condition.[14]

4.2.2 Main Results

Table 3 reports value-weighted time-series returns. The results support the theory on both sides of the model-implied boundary. At short horizons the two groups separate sharply: firms that fail the equity momentum condition in equation (9) (the $\widehat{\mathrm{Cov}}_t < 0$ column) exhibit statistically significant reversal at the one- and two-month horizons (-0.28% and -0.34% per month), whereas firms satisfying the condition (the $\widehat{\mathrm{Cov}}_t > 0$ column) show mild continuation (their returns are positive but insignificant for shorter sorting horizons). In the pooled cross-section (the *All* column), firms failing the condition dominate, and we observe strong reversal. The stronger short-horizon reversal in the unrestricted sample reflects portfolio composition: the *All* strategy is formed separately and is not a weighted average of the two conditional portfolios.

The difference between the two groups is positive and largest at intermediate horizons: at the six-month formation horizon, firms in the $\widehat{\mathrm{Cov}}_t > 0$ column earn 0.81% per month against mild reversal for firms in the $\widehat{\mathrm{Cov}}_t < 0$ column, a statis-

[14] This interpretation is most accurate when the two groups have similar persistence and dispersion in expected returns and similar return volatility.

tically significant difference of 0.84% per month ($t = 3.83$). At the twelve-month horizon the separation narrows. Firms satisfying the equity momentum condition still earn 0.74% per month, but firms failing the condition also earn a significant 0.30% per month, so the difference falls to 0.45% ($t = 1.94$).

Consistent with this horizon effect, even at the noisy one-month horizon, firms in the $\widehat{\text{Cov}}_t < 0$ column reverse significantly while firms in the $\widehat{\text{Cov}}_t > 0$ column display mild continuation. At longer horizons, both groups earn positive returns as persistent expected-return sorting becomes more important. The *Diff* column nets out this common component and remains positive at every horizon and statistically significant beyond one month.

4.2.3 Robustness

Parameter choice. Table IA.1 shows that the results are robust to the parameter choices. The spread between the firms in the $\widehat{\text{Cov}}_t > 0$ and $\widehat{\text{Cov}}_t < 0$ columns is economically large regardless of the chosen parameters.

Risk adjustment. The results survive standard risk adjustments (Table 4). Under both the Fama-French three- and five-factor models (FF3 and FF5), continuation remains concentrated among firms satisfying the equity time-series momentum condition. At the six-month horizon, the FF5 alpha is 0.73% per month for firms satisfying the condition and essentially zero for firms that fail it. At the twelve-month horizon, the alpha remains large for firms satisfying the condition, while firms that fail it also earn a smaller but significant alpha. The condition thus captures variation in momentum that is not explained by conventional factor exposures.

Longer holding horizons. Examining longer holding horizons strengthens the separation (Table 5). With a six-month formation period and a six-month holding

period, firms in the $\widehat{\text{Cov}}_t > 0$ column earn cumulative momentum profits of 3.85% against 1.04% for firms in the $\widehat{\text{Cov}}_t < 0$ column, a significant difference of 2.92% ($t = 4.20$). The return continuation identified by the equity time-series momentum condition therefore persists at longer holding horizons rather than quickly reversing.

Low-leverage, low-variance subsample. Table 6 restricts the sample to firms with leverage below 5% and estimated input volatility $\sqrt{V}$ below 50%, the region where the theory predicts reversal. The cutoffs are read off Figure 1: they place the subsample deep inside the reversal region of the leverage-variance state space, comfortably below the model boundary, so that estimation error in the inputs cannot move firms across it. The choice is conservative rather than unique – any pair of cutoffs well inside the reversal region asks the same question. By construction essentially no firms in this region satisfy the equity time-series momentum condition, so the $\widehat{\text{Cov}}_t > 0$ and *Diff* columns are empty. This is the model's reversal prediction tested directly, and it is confirmed: the firms in this region exhibit significant reversal at the one- to three-month horizons (-0.46%, -0.33%, -0.31% per month, all with $t < -2$) and no significant momentum at longer horizons. This is precisely the leverage-channel pattern the model predicts outside the high-leverage, high-variance region. It confirms that time-series momentum requires a combination of leverage and variance-risk exposure that is sufficient for the variance channel to dominate; otherwise, the leverage channel prevails and returns reverse.

Robustness to leverage–volatility sorting. We next ask whether the equity time-series momentum condition carries information about return continuation beyond the firm characteristics that are known to concentrate momentum. This distinction matters because the model predicts a sign reversal at a model-implied boundary, rather than simply stronger continuation as leverage and variance rise.

Cross-sectionally, the condition is by construction a function of leverage and the input variance, so the question is not whether it depends on these characteristics but whether it merely relabels them. A natural alternative is that $\widehat{\text{Cov}}_{it}$ provides no information beyond leverage and asset variance, or characteristics such as credit rating (Avramov, Chordia, Jostova, and Philipov, 2007). To address this, we sort firms each month into an independent 2×3 grid on leverage and asset volatility, and within each cell compute the value-weighted time-series momentum spread both ignoring the condition and as the difference between condition-satisfying and condition-failing firms. Table 7 shows the condition is not a relabeling. The difference is positive at every horizon, implying that the condition retains predictive information within the portfolios. Within leverage-volatility bins, the condition therefore carries information about which firms continue that the characteristics alone do not.

Controlling for alternative momentum drivers. Finally, if the condition were merely a repackaging of these characteristics, its interaction with past returns should lose significance once past returns are allowed to interact with the characteristics directly. We therefore estimate the regression

$$\begin{aligned} r_{i,t+1} &= \alpha + \beta_1\, r^e_{i,t-h:t} + \beta_2\, \mathbf{1}\{\text{Cov}_{it} > 0\} + \beta_3\, r^e_{i,t-h:t} \times \mathbf{1}\{\text{Cov}_{it} > 0\} \\ &+ \sum_c \delta_1^c\, z_{cit} + \sum_c \delta_2^c\, r^e_{i,t-h:t} \times z_{cit} + \sum_k \gamma_k x_{kit} + \varepsilon_{i,t+1}, \end{aligned} \tag{21}$$

where $r^e_{i,t-h:t}$ is the past h-month excess return, $\mathbf{1}\{\text{Cov}_{it} > 0\}$ indicates whether firm i satisfies the momentum condition, $z_{cit} \in \{\text{log-leverage, asset volatility, credit rating}\}$ denotes the firm characteristics underlying or closely related to the condition, and x_{kit} includes controls for size, value, profitability, turnover, analyst coverage, and industry effects. We interact past returns with the indicator, rather than with the

continuous covariance estimate, to avoid a mechanical link between the level of $\widehat{\text{Cov}}_{it}$ and the estimated sensitivity to past returns. We set $h = 12$ months.

Table 8 reports the results. Column (1) excludes the characteristic interactions $r^e \times z_c$; columns (2)–(4) introduce them one at a time and column (5) includes them jointly, allowing the model-implied interaction β_3 to compete directly with continuation associated with leverage, volatility, and credit rating. The interaction between past returns and the covariance indicator remains positive and significant in every specification, and it is essentially unchanged when past returns are allowed to interact with the characteristics directly. Its magnitude changes only modestly, from 0.009 ($t = 3.04$) without characteristic interactions to 0.007 ($t = 2.74$) in the fully saturated specification, where past returns interact simultaneously with leverage, asset volatility, and credit rating. In that saturated specification, the leverage interaction is also positive and significant (0.005, $t = 2.50$). This is consistent with the model, since leverage is one of the two inputs underlying the equity time-series momentum condition and should therefore capture part of the continuation effect. The relevant result is not that the underlying characteristics contain no information, but that the interaction with the covariance indicator remains economically and statistically stable after accounting for them directly. The continuation identified by the condition therefore cannot be reduced to past returns loading separately on leverage, volatility, or credit rating. Rather, the location of the model-implied boundary – and not merely the characteristics that determine it – contains distinct information about which firms exhibit return continuation.

4.3 Time-Series Momentum in U.S. Corporate Bonds

We next test the model's prediction that corporate bonds should reverse rather than continue. The theory implies that the variance channel that can generate equity momentum works in the opposite direction for debt. As a result, the model predicts that the covariance in equation (16) is generally negative, implying bond return reversal. We examine this prediction using a comprehensive sample of U.S. corporate bonds from TRACE over the period 2002–2024. To obtain reliable return measures, we use the corporate bond return data available through WRDS, constructed following Dick-Nielsen, Feldhütter, Pedersen, and Stolborg (2026).

Table 9 provides a direct test of this prediction. We sort bonds on their own past returns using standard time-series momentum signals and examine subsequent excess returns. Across all formation horizons, bond returns reverse. Long-short returns are negative, ranging from −20 to −40 basis points per month. Moreover, the estimated $\widehat{\mathrm{Cov}}_t(dg^D, r^D)/dt$ is negative in every firm-month, so the condition never identifies positive bond-level return continuation.[15] The model therefore predicts reversal throughout the sample, which is precisely what we observe. This result highlights the central asymmetry of the mechanism. Although the same firms may exhibit strong momentum in equity, their bonds reverse. The variance channel that can generate continuation in equity thus operates in the opposite direction for corporate debt, generating reversal instead.

[15] Accordingly, the $\widehat{\mathrm{Cov}}_t > 0$ column of Table 9 is empty. The *All* and $\widehat{\mathrm{Cov}}_t < 0$ columns differ marginally because the pooled column also includes the few firm-months for which the covariance cannot be evaluated due to missing inputs; no classified firm-month has a positive estimated covariance.

4.4 Equity-to-Bond Momentum Spillover

The model predicts that past equity returns positively predict future bond returns when the spillover covariance, $\widehat{\mathcal{S}}_t = \widehat{\mathrm{Cov}}_t(dg^D, r)$, is positive. We test this prediction by sorting firms according to the spillover condition and constructing firm-level bond time-series momentum portfolios using past *equity* returns as the signal.

Figure 4 plots the fraction of firms satisfying the equity-to-bond spillover condition over the 1966–2024 period. Because spillover imposes a more demanding restriction than the equity time-series momentum condition, the fraction is smaller, averaging only a few percent. It nevertheless varies substantially over time and rises during periods of market stress. After increasing through the early 1970s, the fraction peaks at nearly 6% during the 1973–75 downturn. It then fluctuates between roughly 1% and 3.5% throughout the 1980s and 1990s, with surges around the 1987 crash and the early-1990s recession. The fraction rises again to about 3% during 2000–03 and reaches its sample maximum of approximately 12% in 2009, at the trough of the financial crisis. It remains elevated thereafter, spiking to nearly 7% during the 2020–21 pandemic before declining toward 1% by the end of the sample.

Table 10 reports the spillover results. The pattern predicted by the model is present throughout: firms satisfying the condition, reported in the $\widehat{\mathcal{S}}_t > 0$ column, earn much higher bond returns than firms that do not. At the one-month horizon, the condition-satisfying portfolio earns 1.05% per month, compared with 0.15% for the remaining firms, yielding a difference of 0.87%. The spread remains large at the two-month horizon and gradually declines as the formation horizon lengthens.[16]

The spillover is strongest at the one- and two-month horizons and decays there-

[16] Appendix Table IA.2 shows the results are robust to using bond returns that include accrued interest.

after, consistent with the structure of the condition. The spillover covariance links the contemporaneous equity shock to the innovation in expected bond returns, so it governs the effect of a recent return shock rather than the persistent level of expected returns. A short-horizon equity signal is dominated by that recent shock and therefore aligns with the object the condition describes. As the horizon lengthens, however, the signal increasingly reflects accumulated expected-return drift and earlier shocks, which the contemporaneous condition does not govern. The decay across horizons is therefore the counterpart of the equity own-momentum case: in both settings, the model's sign prediction is sharpest at short horizons, while longer lookbacks increasingly load on persistent expected-return differences. For spillover, this shift dilutes the recent equity shock on which the condition is based.

A potential confounding factor is bond illiquidity. In thinly traded bonds, stale prices and bid–ask bounce can generate spurious return predictability. To address this possibility, we measure liquidity from the cleaned TRACE transactions used to construct bond returns.[17] For each bond-month, we calculate two standard liquidity proxies – the Amihud (2002) price-impact measure and the fraction of zero-trading days – and aggregate them to the firm level using value weights, consistent with the construction of firm-level bond returns. We then average the two firm-level liquidity measures. Each month, firms are sorted into liquid, medium, and illiquid terciles based on lagged liquidity. Table 11 reports the spillover results within each tercile. If the effect were driven by illiquidity, it should be concentrated among illiquid bonds and disappear in the liquid tercile. Instead, the condition-satisfying portfolio in column $\widehat{\mathcal{S}}_t > 0$ earns a positive and significant spillover among the most liquid bonds, where concerns about stale pricing are weakest. The effect is also present

[17] We apply the same cleaning procedure as in Dick-Nielsen, Feldhütter, Pedersen, and Stolborg (2026).

across all three liquidity groups rather than confined to the illiquid tail. Although point estimates are larger among illiquid bonds, consistent with illiquidity amplifying measured returns, the effect does not originate there. The evidence therefore does not support a pure stale-price or illiquidity explanation: the spillover survives among liquid, frequently traded bonds and is not an artifact of the illiquid tail.

The spillover condition is constructed from firm-level inputs at a fixed horizon and therefore identifies which firms should exhibit spillover, rather than which individual bonds. The effect should consequently extend across bonds of different maturities. Splitting the sample by maturity provides a useful check that the firm-level result is not driven by aggregating each firm's bonds into a single return. Table 12 reports the results separately for short-, medium-, and long-maturity bonds at the one- and two-month formation horizons. The spillover is positive in all three maturity groups, and the return difference between the condition-satisfying and remaining portfolios is broadly similar across maturities.

The model yields a sharper prediction for credit quality than for maturity. The variance component of the spillover covariance increases with leverage and equity's exposure to variance risk, both of which become negligible for safe firms whose bonds are close to risk-free. Spillover should therefore be concentrated among speculative-grade issuers, where leverage and default risk are greatest, and weaken as credit quality improves. Table 13 reports results by credit rating. Spillover is concentrated among speculative-grade bonds: the sort produces a significant return difference of approximately 0.90% per month for high-yield issuers. By contrast, the differences among investment-grade bonds are smaller and statistically insignificant, becoming slightly negative for the safest bonds. This pattern is consistent with the model: spillover is strongest where leverage and default risk matter most for bond valuation.

The concentration among speculative-grade issuers is consistent with the positive spillover spreads across liquidity and maturity groups in Tables 11 and 12. Because these tables partition bonds by liquidity and maturity rather than by credit quality, each group can contain the speculative-grade issuers for which the model predicts the strongest spillover. Table 13 isolates the credit-rating dimension and shows that the spread is generated primarily among speculative-grade issuers, where leverage and variance exposure are greatest. Thus, the liquidity and maturity splits show that spillover is not confined to a particular market segment, while the rating split identifies the credit-risk region in which it is strongest.

Taken together, the evidence supports the model's central prediction. Corporate bonds reverse when sorted on their own past returns, yet past equity returns positively predict future bond returns among firms satisfying the model-implied spillover condition. Thus, the same variance channel that generates own-return reversal in bonds also produces economically large equity-to-bond spillover. Consistent with the model, this effect is concentrated among speculative-grade issuers, for which leverage, default risk, and the option-like component of equity are most pronounced.

5 Momentum Crashes

The same firm-level exposures that generate momentum and reversal can also create portfolio-level crash vulnerability. When a large fraction of firms satisfy the momentum condition, common exposures become increasingly important for momentum profits, and the winner-minus-loser portfolio inherits the systematic risk of the firms that generate momentum. We show how asymmetries in common-shock exposures between winners and losers translate these firm-level exposures into momentum-crash risk and derive corresponding empirical measures.

5.1 Momentum Portfolios

Throughout this section, winners and losers refer to the extreme portfolios of a conventional cross-sectional momentum sort. Let $\mathcal{W}_t$ and $\mathcal{L}_t$ denote the winner and loser portfolios, each containing N firms. We assume aggregate shocks are common across firms and retain the common parameters in (4)–(5). Realized firm-level returns contain an idiosyncratic component, not modeled in Section 3 , that is uncorrelated across firms and with aggregate shocks.

Each firm's realized return can be decomposed into components driven by aggregate asset and variance shocks and an idiosyncratic component. Exposure to aggregate shocks is governed by the same elasticities η_i^A, η_i^V that determine the firm's expected return. Averaging across the N firms in each portfolio leg, winner and loser returns therefore load on the common shocks as

$$\begin{aligned} r^{\mathcal{W}} &= \left(r_f + \eta^A_{\mathcal{W}}(\mu - r_f) + \eta^V_{\mathcal{W}}\lambda_V\right) dt + \Delta^A_{\mathcal{W}}\, dW^{A,agg} + \Delta^V_{\mathcal{W}}\, dW^{V,agg} + \varepsilon^{\mathcal{W}}, \quad (22) \\ r^{\mathcal{L}} &= \left(r_f + \eta^A_{\mathcal{L}}(\mu - r_f) + \eta^V_{\mathcal{L}}\lambda_V\right) dt + \Delta^A_{\mathcal{L}}\, dW^{A,agg} + \Delta^V_{\mathcal{L}}\, dW^{V,agg} + \varepsilon^{\mathcal{L}}, \quad (23) \end{aligned}$$

where $\eta^A_{\mathcal{W}}$ and $\eta^V_{\mathcal{W}}$ denote the average asset and variance elasticities of the winner portfolio, with $\Delta^A_{\mathcal{W}} = \frac{1}{N}\sum_{i\in\mathcal{W}} \sigma_A \eta_i^A = \sigma_A\, \eta^A_{\mathcal{W}}$ and $\Delta^V_{\mathcal{W}} = \frac{1}{N}\sum_{i\in\mathcal{W}} \sigma_V \frac{\eta_i^V}{\sqrt{V_i}}$, and analogously for the loser portfolio $\mathcal{L}$. The terms $\varepsilon^{\mathcal{W}}$ and $\varepsilon^{\mathcal{L}}$ are diversifiable idiosyncratic components whose variances are of order $1/N$. The return on the momentum strategy, $r^M = r^{\mathcal{W}} - r^{\mathcal{L}}$, therefore satisfies

$$\begin{aligned} r^M &= \mu^M\, dt + \Delta^A\, dW^{A,agg} + \Delta^V\, dW^{V,agg} + \varepsilon^M, \quad (24) \\ \mu^M &= (\eta^A_{\mathcal{W}} - \eta^A_{\mathcal{L}})(\mu - r_f) + (\eta^V_{\mathcal{W}} - \eta^V_{\mathcal{L}})\lambda_V, \quad (25) \\ \Delta^A &= \Delta^A_{\mathcal{W}} - \Delta^A_{\mathcal{L}}, \qquad \Delta^V = \Delta^V_{\mathcal{W}} - \Delta^V_{\mathcal{L}}, \quad (26) \end{aligned}$$

where $\varepsilon^M = \varepsilon^{\mathcal{W}} - \varepsilon^{\mathcal{L}}$. Conditional on the information available at time t, r^M is Gaussian, with conditional mean $\mu^M\,dt$ and variance

$$\mathrm{Var}_t(r^M) = \left((\Delta^A)^2 + (\Delta^V)^2 + 2\rho^{agg}\,\Delta^A\Delta^V\right)dt + \frac{2\sigma_\varepsilon^2}{N}\,dt, \tag{27}$$

where ρ^{agg} denotes the correlation between the aggregate shocks $dW^{A,agg}$ and $dW^{V,agg}$, and σ_ε^2 the variance of the idiosyncratic components.

A momentum crash is a large negative realization of r^M. Equation (24) shows how asymmetries in the aggregate-shock exposures of winners and losers translate common shocks into momentum returns. We consider the two exposure asymmetries in turn. The first is the asset-loading asymmetry. When losers are more levered than winners, $\eta^A_{\mathcal{L}} > \eta^A_{\mathcal{W}}$, implying $\Delta^A < 0$, a positive aggregate asset shock, $dW^{A,agg} > 0$, lowers the momentum return. During a market rebound, the loser leg rises more than the winner leg, leaving the strategy effectively short the market. The second is the variance-loading asymmetry, which can either amplify or dampen this loss. A higher winner-side variance elasticity raises Δ^V toward positive values. Because rebounds typically coincide with declines in aggregate variance, $dW^{V,agg} < 0$ when $\rho^{agg} < 0$, a positive Δ^V further reduces r^M. The opposite occurs when losers have the larger variance elasticity, so that $\Delta^V < 0$: falling variance then cushions the loss in the particular rebound realization.

This directional effect is distinct from the contribution of Δ^V to overall crash risk, which depends on the full conditional distribution of r^M. Equation (27) characterizes the conditional variance of r^M across all possible realizations of the aggregate shocks, rather than only during a rebound accompanied by falling variance. In that equation, Δ^V enters both through $(\Delta^V)^2$ and through the covariance term $2\rho^{agg}\Delta^A\Delta^V$, so its effect on conditional variance is not invariant to its sign. A more negative Δ^V

widens the distribution when $\Delta^V + \rho^{agg}\Delta^A < 0$, as under our calibration. Holding the conditional mean fixed, a larger loser-side variance loading can therefore reduce the loss in a typical rebound while still increasing the probability of an extreme negative realization by widening the distribution of momentum returns.

A complementary predictor of crash risk is the fraction ω_t of firms satisfying the equity time-series momentum condition. A high value of ω_t indicates that the state associated with large winner–loser differences in leverage and variance exposure is widespread across the cross-section. In such states, losers are likely to become substantially more levered and option-like than winners, making $|\Delta^A|$ and $|\Delta^V|$ correspondingly large. We therefore use ω_t as an additional, empirically motivated predictor of crash risk that captures the breadth of the state generating these asymmetries, rather than as a term entering equation (27) directly.[18]

Table 14 reports partial comparative statics for the four portfolio elasticities, quantifying how crash risk varies with each one. We hold three of $\{\eta^A_{\mathcal{W}}, \eta^A_{\mathcal{L}}, \eta^V_{\mathcal{W}}, \eta^V_{\mathcal{L}}\}$ fixed at their empirical cross-sectional medians ($\eta^A_{\mathcal{L}} = 1.500$, $\eta^A_{\mathcal{W}} = 1.250$, $\eta^V_{\mathcal{L}} = 0.025$, and $\eta^V_{\mathcal{W}} = 0.015$) and vary the fourth across percentiles of its empirical distribution. For each configuration we simulate 100,000 monthly draws from (24) under the calibration $\mu - r_f = 4\%$, $\lambda_V = -1.75$, $\sigma_A = 20\%$, $\sigma_V = 80\%$, $\rho^{agg} = -0.15$, and report the probability of a crash, defined as $r^M_{t+1} < -11\%$. Relative to the baseline calibration, the aggregate-shock volatilities are increased to reflect the high-volatility states in which momentum crashes tend to occur (Daniel and Moskowitz, 2016). Because these volatilities are common to both legs, the only source of asymmetry between winners and losers is the empirically measured difference in their elasticities.

[18] The two components in μ^M work in opposite directions. More levered losers lower μ^M through the asset term $(\eta^A_{\mathcal{W}} - \eta^A_{\mathcal{L}})(\mu - r_f) < 0$, whereas more option-like losers raise it through the variance term $(\eta^V_{\mathcal{W}} - \eta^V_{\mathcal{L}})\lambda_V > 0$. When the variance term dominates, states with high expected momentum may therefore also be states in which a large fraction of firms satisfies the momentum condition.

The main object of interest is therefore the comparative pattern across the four elasticities, which is robust to alternative choices of aggregate volatility.

Two results stand out. First, crash probability is sensitive to losers' asset elasticity and winners' variance elasticity. For instance, increasing $\eta^A_{\mathcal{L}}$ from its median value of 1.5 to its 98th percentile raises the crash probability from essentially zero to 3.4%. Second, crash probabilities respond only weakly to winners' asset elasticity or losers' variance elasticity. These are precisely the two asymmetries the model identifies: a higher $\eta^A_{\mathcal{L}}$ makes Δ^A more negative, increasing the strategy's short-rebound exposure, while a higher $\eta^V_{\mathcal{W}}$ makes Δ^V more positive, increasing its exposure to the decline in variance that typically accompanies a rebound. By contrast, changes in $\eta^A_{\mathcal{W}}$ or $\eta^V_{\mathcal{L}}$ move the corresponding loadings in the opposite direction and have little net effect on crash probabilities. Crash risk therefore reflects the asymmetry between winners and losers, rather than the level of any single elasticity in isolation.

A caveat concerns the interpretation of these comparative statics. Each panel varies one elasticity while holding the other three fixed at their medians, thereby isolating its partial effect under the chosen calibration. In particular, Panel D increases winners' variance elasticity $\eta^V_{\mathcal{W}}$ into a range that is empirically more characteristic of losers than winners. In the data, however, the two legs do not vary independently. Losers are systematically more levered *and* more option-like than winners, so they tend to dominate both the asset and the variance loadings. Panel D should therefore be interpreted as illustrating the underlying comparative static, rather than as representing the joint configuration typically observed in the data.

5.2 Empirical Evidence

We next test the model's predictions for momentum crashes. We define a momentum crash as an indicator equal to one when the value-weighted winner-minus-loser return falls below -11%. This threshold corresponds to the bottom 5% of the return distribution over 1966–2024 and captures the worst 35 monthly realizations in the sample. We estimate

$$\Pr(\text{Crash}_{t+1} = 1) = \Lambda(\alpha_k + \beta_k X_{k,t} + \gamma_{1,k} R^{mkt}_{t-24:t} + \gamma_{2,k} Vol^{mkt}_{t-6:t}), \tag{28}$$

using a logit model with heteroskedasticity-robust standard errors, where Λ is the logistic function, $X_{k,t} \in \{\mu^M,\ \omega_t,\ \Delta^A,\ \Delta^V\}$, μ^M is the model-implied expected momentum return from (25), ω_t is the fraction of firms satisfying the momentum condition, and Δ^A, Δ^V are the momentum strategy's exposures to aggregate asset and variance shocks. Each model variable enters in a separate specification, and all specifications control for the conditioning information behind the crash predictors of Daniel and Moskowitz (2016): the past 24-month market return $R^{mkt}_{t-24:t}$, underlying their bear-market indicator, and the trailing 6-month market volatility $Vol^{mkt}_{t-6:t}$, underlying their ex ante variance measure.

To construct μ^M, Δ^A, and Δ^V we compute the equal-weighted averages of the firm-level elasticities η^A and η^V within the winner and loser deciles, using the same firm-level estimates as in Section 4.2. The aggregate shock loadings scale these averages by the calibrated volatilities, $\Delta^A_{\mathcal{W}} = \sigma_A\, \eta^A_{\mathcal{W}}$ and $\Delta^V_{\mathcal{W}} = \sigma_V\, (\eta^V_{\mathcal{W}}/\sqrt{V})$ with analogous definitions for the loser leg. The momentum strategy's aggregate-shock exposures are therefore $\Delta^A = \Delta^A_{\mathcal{W}} - \Delta^A_{\mathcal{L}}$ and $\Delta^V = \Delta^V_{\mathcal{W}} - \Delta^V_{\mathcal{L}}$.

Panel A of Table 15 shows that momentum crashes are predictable in sample.

The fraction of firms satisfying the momentum condition, ω_t, positively predicts subsequent crashes. A broad base of condition-satisfying firms signals synchronized distress across the cross-section, when winner–loser differences in leverage and variance exposure, and hence $|\Delta^A|, |\Delta^V|$, are particularly pronounced. This pattern is visible in Figure 3, where ω_t spikes around several of the largest momentum-crash episodes, reaching nearly 40% in 2009 and rising sharply in 1974–75, 2001, and 2020–21. These are post-drawdown, high-volatility states in which losers are particularly levered and the strategy is especially exposed to a rebound. The economic magnitude is substantial. Although the unconditional crash frequency is 5%, moving ω_t from the 5–15% band that prevails in normal times (Figure 3) to the 25–40% levels reached in major downturns raises the predicted crash probability to approximately 15–20%. The breadth of the momentum condition therefore carries economically meaningful information about future crash risk.

The model-implied expected momentum return μ^M also positively predicts subsequent crashes. This finding is consistent with the model because high-μ^M states tend to coincide with a large fraction of firms satisfying the momentum condition and with greater common systematic exposure in the winner-minus-loser portfolio. High expected momentum returns therefore signal not only greater prospective profitability but also greater vulnerability to a crash.

Columns (3) and (4) line up directly with the aggregate-shock mechanism. Both the asset-shock asymmetry Δ^A and the variance-shock asymmetry Δ^V enter negatively and significantly: crashes become more likely as the winner-minus-loser portfolio's exposure to common asset and variance shocks becomes more negative. Because losers are more levered and more option-like than winners, both Δ^A and Δ^V are negative on average. The asset channel operates through direct short-rebound

exposure: a positive asset shock lowers r^M. The variance channel is more subtle. During a rebound, when $\rho^{agg} < 0$ implies falling aggregate variance, a negative Δ^V cushions the loss by raising r^M. At the same time, Δ^V also affects the conditional variance of r^M through equation (27) and for the magnitudes in our calibration this variance rises with $|\Delta^V|$. A crash is a left-tail event of a Gaussian, so the wider distribution raises crash probability even though the same term cushions the mean loss in the specific rebound scenario. These effects remain significant after controlling for the predictors of Daniel and Moskowitz (2016), suggesting that ω_t, Δ^A, and Δ^V contain information beyond that captured by past market returns and volatility. Momentum crashes are therefore associated not only with market rebounds, but also with the endogenous risk exposures implied by the model.

Panel B examines the winner and loser legs to assess where predictability is concentrated. Both elasticity spreads, $\eta^A_{\mathcal{W}} - \eta^A_{\mathcal{L}}$ and $\eta^V_{\mathcal{W}} - \eta^V_{\mathcal{L}}$, enter negatively and significantly, indicating that crash risk rises as losers become more sensitive than winners to aggregate asset and variance shocks. Examining the two legs separately sharpens this result. Losers' asset loading, $\Delta^A_{\mathcal{L}}$, strongly predicts crashes, whereas winners' asset loading, $\Delta^A_{\mathcal{W}}$, is weak. The same pattern holds for variance: losers' variance loading, $\Delta^V_{\mathcal{L}}$, is a strong predictor, while winners' loading, $\Delta^V_{\mathcal{W}}$, carries little explanatory power.[19] Both channels are therefore concentrated in the short leg. Losers' asset loading raises crash risk directly by deepening the short-rebound exposure. Losers' variance loading operates differently. During a rebound accompanied by falling variance, it cushions the loss because the negative variance loading raises r^M. At the same time, it increases the conditional variance of r^M through equation (27). It is this widening of the return distribution, rather than a directional

[19] Note that Table 14 isolates one elasticity at a time, while the empirical regressions place more weight on losers' variance loading because leverage and variance exposure move jointly in the data.

exposure to the rebound, that raises the probability of a left-tail crash.

Overall, these findings are consistent with the portfolio-level implications developed in Section 5.1, which build on the paper's firm-level mechanism. Momentum-crash risk is elevated when the short leg becomes more exposed to common shocks, creating large asymmetries between winners and losers in their asset and variance loadings. Market rebounds remain an important part of the mechanism, as in Daniel and Moskowitz (2016), while the cross-sectional structure of winner–loser exposures provides explanatory power beyond aggregate market returns and volatility.

6 Conclusion

This paper develops a unified framework linking equity time-series momentum and reversal, corporate bond reversal, equity-to-bond return spillovers, and momentum crashes. Using the Merton (1974) framework as a valuation map, we treat variance as a priced state variable and show that return dynamics reflect two opposing forces. The leverage channel generates reversal by increasing expected returns following poor performance, while the variance channel generates continuation by increasing exposure to priced variance risk. Momentum arises when the variance channel dominates, while reversal arises when the leverage channel dominates.

The model yields a firm-level condition that identifies when realized equity returns and innovations in expected returns move in the same direction. Consistent with this prediction, firms satisfying the condition exhibit economically large and statistically significant time-series momentum, while firms failing the condition reverse. In the low-leverage, low-variance region, where the leverage channel necessarily dominates, the data show precisely the strong reversal predicted by the model.

The framework also generates novel predictions across firms' capital structures.

Because debt is a concave claim on firm value, the variance channel that generates momentum in equity operates in the opposite direction for corporate bonds. The model therefore predicts reversal rather than continuation in debt, and the data bear this out. Bond time-series momentum is significantly negative across horizons. At the same time, shared exposure to firm-level shocks implies that past equity returns can positively predict future bond returns. Consistent with this prediction, we find economically large equity-to-bond spillovers concentrated among firms satisfying the model-implied spillover condition, even though the bonds of those firms reverse when sorted on their own past returns.

Finally, the model speaks to momentum crashes. When past losers become substantially more levered than past winners, momentum portfolios acquire greater negative exposure to aggregate rebounds. Consistent with this mechanism, measures of asset-loading asymmetry and the breadth of the momentum condition significantly predict future crash episodes in sample. Momentum-crash risk can therefore arise from the same firm-level forces that generate momentum and reversal, without additional return nonlinearities.

Taken together, we identify a capital-structure mechanism behind the shock-driven component of time-series return predictability. The findings highlight how leverage, payoff convexity, and variance risk shape return dynamics across securities. In this sense, the paper connects the momentum literature with a growing body of work emphasizing the importance of variance risk in asset prices and expected returns (e.g., Bollerslev, Tauchen, and Zhou, 2009; Du, Elkamhi, and Ericsson, 2019). By showing how priced variance risk interacts with firms' capital structures to generate momentum and reversal, spillover across securities, and momentum crashes, it provides a unified perspective on return predictability across the capital structure.

References

Amihud, Yakov, 2002, Illiquidity and Stock Returns: Cross-Section and Time-Series Effects, *Journal of Financial Markets* 5, 31–56.

Avramov, Doron, Tarun Chordia, Gergana Jostova, and Alexander Philipov, 2007, Momentum and Credit Rating, *Journal of Finance* 62, 2503–2520.

Barroso, Pedro, and Pedro Santa-Clara, 2015, Momentum has Its Moments, *Journal of Financial Economics* 116, 111–120.

Bharath, Sreedhar T., and Tyler Shumway, 2008, Forecasting Default with the Merton Distance to Default Model, *Review of Financial Studies* 21, 1339–1369.

Bollerslev, Tim, George Tauchen, and Hao Zhou, 2009, Expected Stock Returns and Variance Risk Premia, *Review of Financial Studies* 22, 4463–4492.

Carr, Peter, and Liuren Wu, 2009, Variance Risk Premiums, *Review of Financial Studies* 22, 1311–1341.

Carr, Peter, and Liuren Wu, 2020, Option Profit and Loss Attribution and Pricing: A New Framework, *Journal of Finance* 75, 2271–2316.

Chen, Long, Pierre Collin-Dufresne, and Robert S. Goldstein, 2009, On the Relation Between the Credit Spread Puzzle and the Equity Premium Puzzle, *The Review of Financial Studies* 22, 3367–3409.

Choi, Jaewon, and Yongjun Kim, 2018, Anomalies and Market (Dis)integration, *Journal of Monetary Economics* 100, 16–34.

Chordia, Tarun, Amit Goyal, Yoshio Nozawa, Avanidhar Subrahmanyam, and Qing Tong, 2017, Are Capital Market Anomalies Common to Equity and Corporate Bond Markets? An Empirical Investigation, *Journal of Financial and Quantitative Analysis* 52, 1301–1342.

Collin-Dufresne, Pierre, Benjamin Junge, and Anders B. Trolle, 2024, How Integrated are Credit and Equity Markets? Evidence from Index Options, *Journal of Finance* 79, 949–992.

Cremers, K.J. Martijn, Joost Driessen, and Pascal Maenhout, 2008, Explaining the Level of Credit Spreads: Option-Implied Jump Risk Premia in a Firm Value Model, *The Review of Financial Studies* 21, 2209–2242.

Daniel, Kent, and Tobias J. Moskowitz, 2016, Momentum Crashes, *Journal of Financial Economics* 122, 221–247.

Dick-Nielsen, Jens, Peter Feldhütter, Lasse Heje Pedersen, and Christian Stolborg, 2026, Corporate Bond Factors: Replication Failures and a New Framework, Working paper.

Dickerson, Alex, Mathieu Fournier, Kris Jacobs, and Piotr Orlowski, 2026, Systematic Variance Risk Everywhere in Equity Option Markets, Working paper.

Dickerson, Alexander, Mathieu Fournier, Alexandre Jeanneret, and Philippe Mueller, 2025, A Credit Risk Explanation of the Correlation between Corporate Bonds and Stocks, Working paper.

Du, Du, Redouane Elkamhi, and Jan Ericsson, 2019, Time-Varying Asset Volatility and the Credit Spread Puzzle, *Journal of Finance* 74, 1841–1885.

Duarte, Jefferson, Christopher S. Jones, and Junbo L. Wang, 2024, Very Noisy Option Prices and Inference Regarding the Volatility Risk Premium, *The Journal of Finance* 79, 3581–3621.

Fama, Eugene F., and Kenneth R. French, 1993, Common Risk Factors in the Returns on Stocks and Bonds, *Journal of Financial Economics* 33, 3–56.

Fama, Eugene F., and Kenneth R. French, 2008, Dissecting Anomalies, *Journal of Finance* 63, 1653–1678.

Fama, Eugene F., and Kenneth R. French, 2015, A Five-Factor Asset Pricing Model, *Journal of Financial Economics* 116, 1–22.

Fama, Eugene F., and James D. MacBeth, 1973, Risk, Return, and Equilibrium: Empirical Tests, *Journal of Political Economy* 81, 607–636.

Garlappi, Lorenzo, and Hong Yan, 2011, Financial Distress and the Cross-section of Equity Returns, *Journal of Finance* 66, 789–822.

Gebhardt, William R., Soeren Hvidkjaer, and Bhaskaran Swaminathan, 2005, Stock and bond market interaction: Does momentum spill over?, *Journal of Financial Economics* 75, 651–690.

Goyal, Amit, and Narasimhan Jegadeesh, 2018, Cross-Sectional and Time-Series Tests of Return Predictability: What Is the Difference?, *Review of Financial Studies* 31, 1784–1824.

Greenwood, Robin, Samuel G. Hanson, and Gordon Y. Liao, 2018, Asset Price Dynamics in Partially Segmented Markets, *The Review of Financial Studies* 31, 3307–3343.

Herskovic, Bernard, Bryan Kelly, Hanno Lustig, and Stijn Van Nieuwerburgh, 2016, The Common Factor in Idiosyncratic Volatility: Quantitative Asset Pricing Implications, *Journal of Financial Economics* 119, 249–283.

Heston, Steven L., 1993, A Closed-Form Solution for Options with Stochastic Volatility with Applications to Bond and Currency Options, *Review of Financial Studies* 6, 327–343.

Heston, Steven L., and Karamfil Todorov, 2025, The Variance and Return Premiums across Assets, Working paper.

Huang, Dashan, Jiangyuan Li, Liyao Wang, and Guofu Zhou, 2020, Time series momentum: Is it there?, *Journal of Financial Economics* 135, 774–794.

Jegadeesh, Narasimhan, 1990, Evidence of Predictable Behavior of Security Returns, *Journal of Finance* 45, 881–898.

Johnson, Timothy C., 2002, Rational Momentum Effects, *Journal of Finance* 57, 585–608.

Jostova, Gergana, Stanislava Nikolova, Alexander Philipov, and Christoph W. Stahel, 2013, Momentum in Corporate Bond Returns, *Review of Financial Studies* 26, 1649–1693.

Keshavarz, Javad, and Stace Sirmans, 2026, Momentum Across the Capital Structure, Working Paper.

Liu, Laura Xiaolei, and Lu Zhang, 2008, Momentum Profits, Factor Pricing, and Macroeconomic Risk, *Review of Financial Studies* 21, 2417–2448.

McQuade, Timothy J., 2018, Stochastic Volatility and Asset Pricing Puzzles, Working paper.

Mencía, Javier, and Enrique Sentana, 2013, Valuation of VIX derivatives, *Journal of Financial Economics* 108, 367–391.

Merton, Robert C., 1974, On the Pricing of Corporate Debt: The Risk Structure of Interest Rates, *Journal of Finance* 29, 449–470.

Moskowitz, Tobias J., Yao H. Ooi, and Lasse Heje Pedersen, 2012, Time-Series Momentum, *Journal of Financial Economics* 104, 228–250.

Pitkäjärvi, Aleksi, Matti Suominen, and Lauri Vaittinen, 2020, Cross-asset signals and time series momentum, *Journal of Financial Economics* 136, 63–85.

Sagi, Jacob S., and Mark S. Seasholes, 2007, Firm-Specific Attributes and the Cross Section of Momentum, *Journal of Financial Economics* 84, 389–434.

Zhang, Benjamin Y., Hao Zhou, and Haibin Zhu, 2009, Explaining Credit Default Swap Spreads with the Equity Volatility and Jump Risks of Individual Firms, *Review of Financial Studies* 22, 5099–5131.

Zhang, X. Frank, 2006, Information Uncertainty and Stock Returns, *Journal of Finance* 61, 105–136.

Appendix

A Expected Return Sensitivities

The condition for time-series momentum depends on the sensitivities of $\eta_t^A = E_A \frac{A}{E}$ and $\eta_t^V = E_V \frac{V}{E}$ with respect to the model's state variables. That is, it depends on $\frac{\partial \eta_t^A}{\partial A}$, $\frac{\partial \eta_t^V}{\partial A}$, $\frac{\partial \eta_t^A}{\partial V}$ and $\frac{\partial \eta_t^V}{\partial V}$. Throughout, V denotes the input *variance*, consistent with Section 3.1; the volatility is $\sqrt{V}$. We also suppress the arguments from $A(t), V(t)$, and $E(t, A(t), F, V(t), T)$. We define

$$d_1 \equiv \frac{\ln(m) + \frac{V}{2}\tau}{\sqrt{V\,\tau}}, \qquad d_2 \equiv d_1 - \sqrt{V\,\tau}, \qquad m \equiv \frac{A}{Fe^{-\tau r_f}}, \tag{A1}$$

where $\Phi(\cdot)$ is the normal cdf and $\varphi(\cdot)$ the normal pdf. The relevant Black–Scholes sensitivities, expressed with respect to variance, are

$$E_A = \Phi(d_1), \qquad E_V = \frac{A\,\varphi(d_1)\sqrt{\tau}}{2\sqrt{V}}, \tag{A2}$$

where E_V follows from the vega $\partial E/\partial\sqrt{V} = A\varphi(d_1)\sqrt{\tau}$ by the chain rule $\partial E/\partial V = (\partial E/\partial\sqrt{V})\,(2\sqrt{V})^{-1}$.

Sign of $\partial\eta_t^A/\partial A$. We first prove that $\frac{\partial \eta_t^A}{\partial A} < 0$. Note that $E_A = \Phi(d_1)$ is the standard Black–Scholes delta, so

$$\eta_t^A = \Phi(d_1)\frac{A}{E} = \left[\frac{A\Phi(d_1) - Fe^{-\tau r_f}\Phi(d_2)}{A\Phi(d_1)}\right]^{-1} = \left[1 - \frac{1}{m} \times \frac{\Phi(d_2)}{\Phi(d_1)}\right]^{-1}. \tag{A3}$$

Write $\eta_t^A = (1-x)^{-1}$ with $x \equiv \frac{1}{m}\frac{\Phi(d_2)}{\Phi(d_1)}$. Differentiating x with respect to A gives

$$\frac{\partial x}{\partial A} = \frac{\partial}{\partial A}\left(\frac{1}{m}\frac{\Phi(d_2)}{\Phi(d_1)}\right) = \frac{1}{m}\,\frac{\varphi(d_2)\Phi(d_1) - \Phi(d_2)\varphi(d_1) - \Phi(d_1)\Phi(d_2)\sqrt{V\,\tau}}{A\,\Phi(d_1)^2\,\sqrt{V\,\tau}}. \quad \text{(A4)}$$

Applying the chain rule $\frac{\partial \eta_t^A}{\partial A} = (1-x)^{-2}\frac{\partial x}{\partial A}$, we obtain

$$\frac{\partial \eta_t^A}{\partial A} = \frac{\dfrac{1}{m}\,\dfrac{\varphi(d_2)\Phi(d_1) - \Phi(d_2)\varphi(d_1) - \Phi(d_1)\Phi(d_2)\sqrt{V\,\tau}}{A\,\Phi(d_1)^2\,\sqrt{V\,\tau}}}{\left(1 - \dfrac{1}{m}\dfrac{\Phi(d_2)}{\Phi(d_1)}\right)^2}. \quad \text{(A5)}$$

Since $1/m > 0$, $A\Phi(d_1)^2\sqrt{V\,\tau} > 0$, and $\left(1 - \frac{1}{m}\frac{\Phi(d_2)}{\Phi(d_1)}\right)^2 > 0$, the sign of $\frac{\partial \eta_t^A}{\partial A}$ equals the sign of $\varphi(d_2)\Phi(d_1) - \Phi(d_2)\varphi(d_1) - \Phi(d_1)\Phi(d_2)\sqrt{V\,\tau}$.

Factoring out $\Phi(d_1)\Phi(d_2) > 0$, it suffices to prove that

$$\frac{\varphi(d_2)}{\Phi(d_2)} - \frac{\varphi(d_1)}{\Phi(d_1)} < \sqrt{V\,\tau} \quad \text{(A6)}$$

for all d_1 and d_2, which yields $\frac{\partial \eta_t^A}{\partial A} < 0$. For compact notation, let $h(x) \equiv \varphi(x)/\Phi(x)$ and $s \equiv \sqrt{V\,\tau}$. Because $d_1 - d_2 = s$, the bound $h(d_2) - h(d_1) < s$ holds as long as $|h'(d)| < 1$ for all d. Indeed, if $|h'(d)| < 1$ then

$$\int_{d_2}^{d_1} |h'(x)|\,dx < \int_{d_2}^{d_1} 1\,dx = d_1 - d_2 = s, \quad \text{(A7)}$$

and therefore

$$h(d_2) - h(d_1) = \left|\int_{d_2}^{d_1} h'(x)\,dx\right| \leq \int_{d_2}^{d_1} |h'(x)|\,dx < s, \quad \text{(A8)}$$

where the second step is the standard bound on the absolute value of a definite

integral. Thus condition (A6) holds whenever $|h'(d)| < 1$.

To establish $|h'(d)| < 1$, we proceed in three steps. First, we show the preliminary result $h(x)+x > 0$. Second, we use it to show $h'(x) < 0$. Third, we prove $h'(x) > -1$. Together these give $h'(x) \in (-1, 0) \subset (-1, 1)$.

(i) $h(x)+x > 0$. Define $g(x) \equiv \varphi(x)+x\Phi(x)$. By L'Hôpital's rule $\lim_{x\to-\infty} g(x) = 0$, and $g'(x) = -x\varphi(x) + x\varphi(x) + \Phi(x) = \Phi(x) > 0$. Hence g is zero at $-\infty$ and increasing, so $g(x) > 0$; since $\Phi(x) > 0$, $h(x) + x = g(x)/\Phi(x) > 0$.

(ii) $h'(x) < 0$. Differentiating $h = \varphi/\Phi$ gives $h'(x) = -h(x)\,[x + h(x)]$. Since $h(x) > 0$ and $x + h(x) > 0$ by (i), $h'(x) < 0$.

(iii) $h'(x) + 1 > 0$. Define $f(x) \equiv \frac{\varphi'(x)}{\varphi(x)}\Phi(x) - \varphi(x) + \frac{\Phi^2(x)}{\varphi(x)}$. Then

$$\frac{\varphi(x)}{\Phi^2(x)}\, f(x) = \frac{\varphi(x)}{\Phi^2(x)}\left[\frac{\varphi'(x)}{\varphi(x)}\Phi(x) - \varphi(x) + \frac{\Phi^2(x)}{\varphi(x)}\right] = \frac{\varphi'(x)\Phi(x) - \varphi^2(x)}{\Phi^2(x)} + 1 = h'(x)+1. \tag{A9}$$

Since $\varphi'(x) = -x\varphi(x)$,

$$f'(x) = -\Phi(x) - x\varphi(x) + x\varphi(x) + \frac{2\Phi(x)\varphi(x) + x\Phi^2(x)}{\varphi(x)} = \Phi(x)\left[1 + \frac{x}{h(x)}\right]. \tag{A10}$$

Because $h(x) > 0$ and $h(x)+x > 0$, we have $1+\frac{x}{h(x)} > 0$, so $f'(x) > 0$. Together with $\lim_{x\to-\infty} f(x) = 0$, this gives $f(x) > 0$, hence $\frac{\varphi(x)}{\Phi^2(x)} f(x) = h'(x) + 1 > 0$ and $h'(x) > -1$.

Thus $\varphi(d_2)\Phi(d_1) - \Phi(d_2)\varphi(d_1) - \Phi(d_1)\Phi(d_2)\sqrt{V\,\tau} < 0$, so $\frac{\partial \eta_t^A}{\partial A} < 0$. □

Sign of $\partial \eta_t^V / \partial A$. We next prove that

$$\frac{\partial \eta_t^V}{\partial A} = \frac{V(E_{AV}E - E_V E_A)}{E^2} < 0. \tag{A11}$$

Using (A2), equity's variance elasticity can be written as

$$\eta_t^V = E_V \frac{V}{E} = \frac{A_t}{E} \frac{\varphi(d_1)\sqrt{V\,\tau}}{2} = \eta_t^A \frac{\varphi(d_1)}{\Phi(d_1)} \frac{\sqrt{V\,\tau}}{2}. \tag{A12}$$

Hence

$$\frac{\partial \eta_t^V}{\partial A} = \frac{\sqrt{V\,\tau}}{2} \left(\frac{\partial \eta_t^A}{\partial A} \frac{\varphi(d_1)}{\Phi(d_1)} + \eta_t^A \frac{\partial}{\partial A} \left(\frac{\varphi(d_1)}{\Phi(d_1)} \right) \right). \tag{A13}$$

We have $\frac{\sqrt{V\,\tau}}{2} > 0$, $\eta_t^A > 0$, and $\frac{\varphi(d_1)}{\Phi(d_1)} > 0$. Moreover, we proved above that $\frac{\partial \eta_t^A}{\partial A} < 0$, and

$$\frac{\partial}{\partial A} \left(\frac{\varphi(d_1)}{\Phi(d_1)} \right) = -\frac{\varphi(d_1)}{\Phi(d_1)} \left(d_1 + \frac{\varphi(d_1)}{\Phi(d_1)} \right) \frac{1}{A\sqrt{V\,\tau}} < 0, \tag{A14}$$

since $d_1 + \frac{\varphi(d_1)}{\Phi(d_1)} = d_1 + h(d_1) > 0$ by step (i). Both terms in the bracket are therefore negative, confirming $\frac{\partial \eta_t^V}{\partial A} < 0$. □

Sign of $\partial \eta_t^A / \partial V$. The derivative is

$$\frac{\partial \eta_t^A}{\partial V} = \frac{A(E_{AV} E - E_V E_A)}{E^2}, \tag{A15}$$

which is identical to the expression in (A11) except that the leading factor is A rather than V. Since $A > 0$ and $V > 0$, $\frac{\partial \eta_t^A}{\partial V}$ has the same sign as $\frac{\partial \eta_t^V}{\partial A}$ and is therefore strictly negative. □

Sign of $\partial \eta_t^V / \partial V$. Finally,

$$\frac{\partial \eta_t^V}{\partial V} = \frac{E_V + V E_{VV}}{E} - \frac{V E_V^2}{E^2}. \tag{A16}$$

Substituting the variance-convention sensitivities, $\frac{\partial \eta_t^V}{\partial V} > 0$ if

$$\Big(e^n \Phi(d_1) - \Phi(d_2)\Big)\Big(d_1 d_2 + 1\Big) > e^n \sqrt{V\,\tau}\,\varphi(d_1), \tag{A17}$$

with $n = \log\big(Ae^{\tau r_f}/F\big)$. The derivative is negative in very-high-variance states but is more likely to be positive for low-leverage firms ($A \gg F$).

Figures and Tables

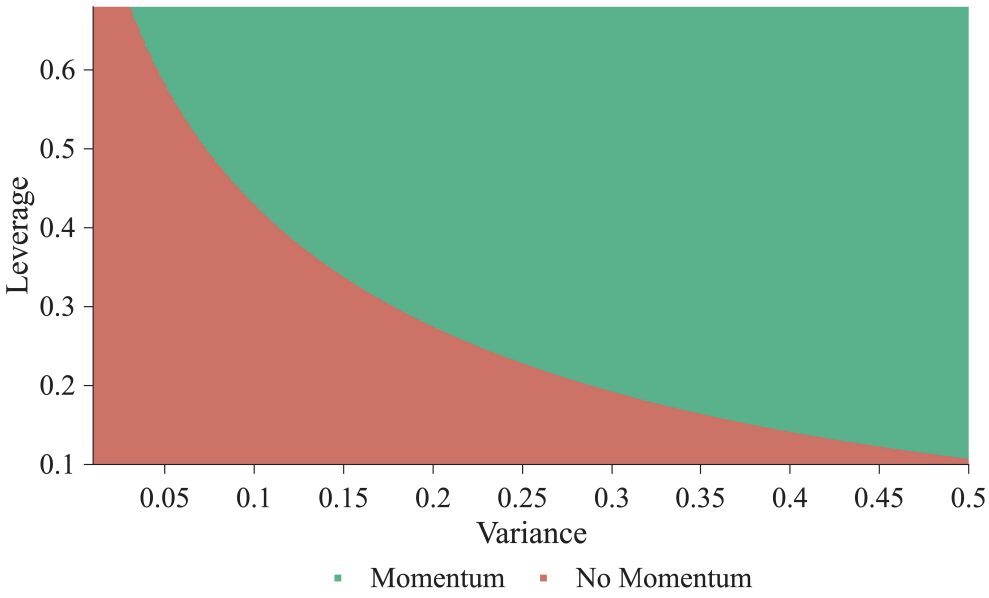

Figure 1
Sensitivity of equity momentum condition
The figure plots the sign of $\mathrm{Cov}_t\left(dg, r\right)$ from equation (12) as a function of leverage F/A and variance V. The green and red areas denote states where $\mathrm{Cov}_t\left(dg, r\right)$ is positive and negative, respectively: a positive covariance implies time-series momentum and a negative covariance implies reversal. We use the following annualized parameters: asset risk premium $\mu - r_f = 4\%$, price of variance risk $\lambda_V = -1.75$, asset volatility $\sigma_A = 0.09$, input variance volatility $\sigma_V = 0.40$, time to maturity $\tau = 1$, and correlation between the asset and input-variance shocks $\rho = -0.15$.

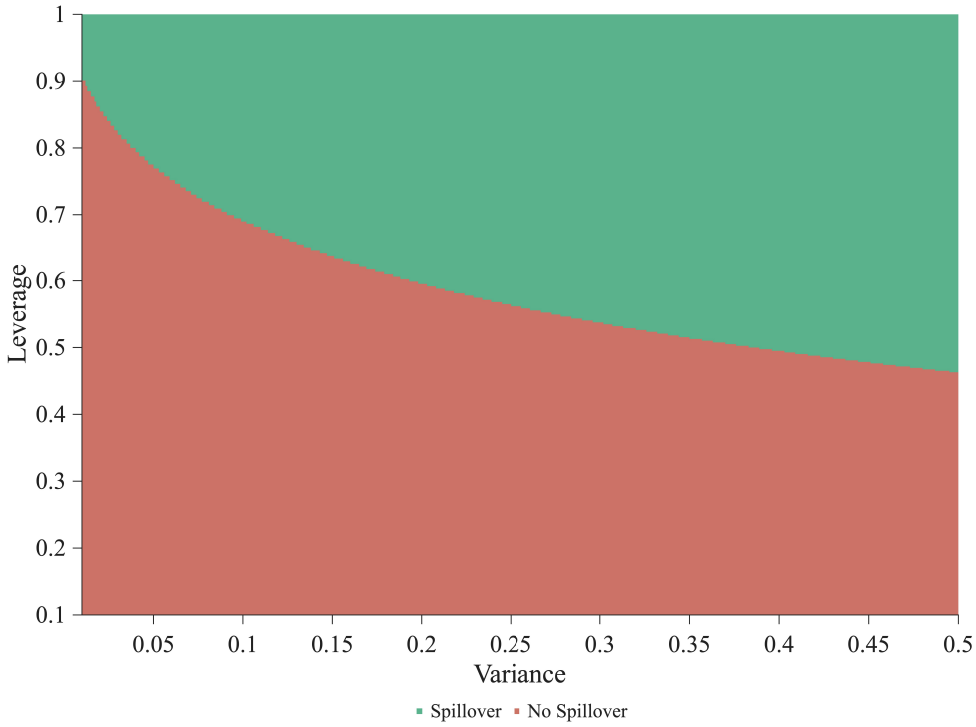

Figure 2
Momentum spillover between past equity and expected bond returns
The figure plots the sign of $\text{Cov}_t\left(dg^D, r\right)$ from equation (18) as a function of leverage F/A and variance V. The green and red areas denote states where $\text{Cov}_t\left(dg^D, r\right)$ is positive and negative, implying positive equity-to-bond momentum spillover and no momentum spillover, respectively. We use the following annualized parameters: asset risk premium $\mu - r_f = 4\%$, price of variance risk $\lambda_V = -1.75$, asset volatility $\sigma_A = 0.09$, input variance volatility $\sigma_V = 0.40$, time to maturity $\tau = 1$, and correlation between the asset and input-variance shocks $\rho = -0.15$.

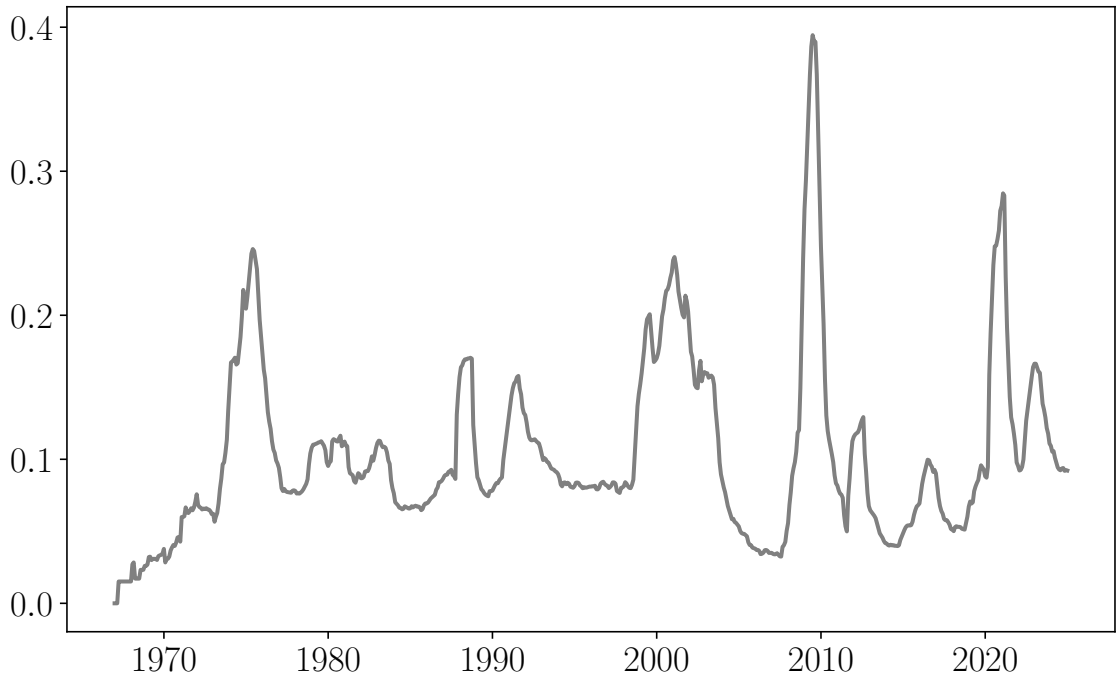

Figure 3
Fraction of firms with equity time-series momentum
The figure plots the monthly fraction of firms satisfying the equity time-series momentum condition in equation (9), evaluated using the estimated model-implied covariance, $\widehat{\mathrm{Cov}}_t(dg, r)$, from equation (12), over 1966–2024. The series is smoothed using a twelve-month moving average.

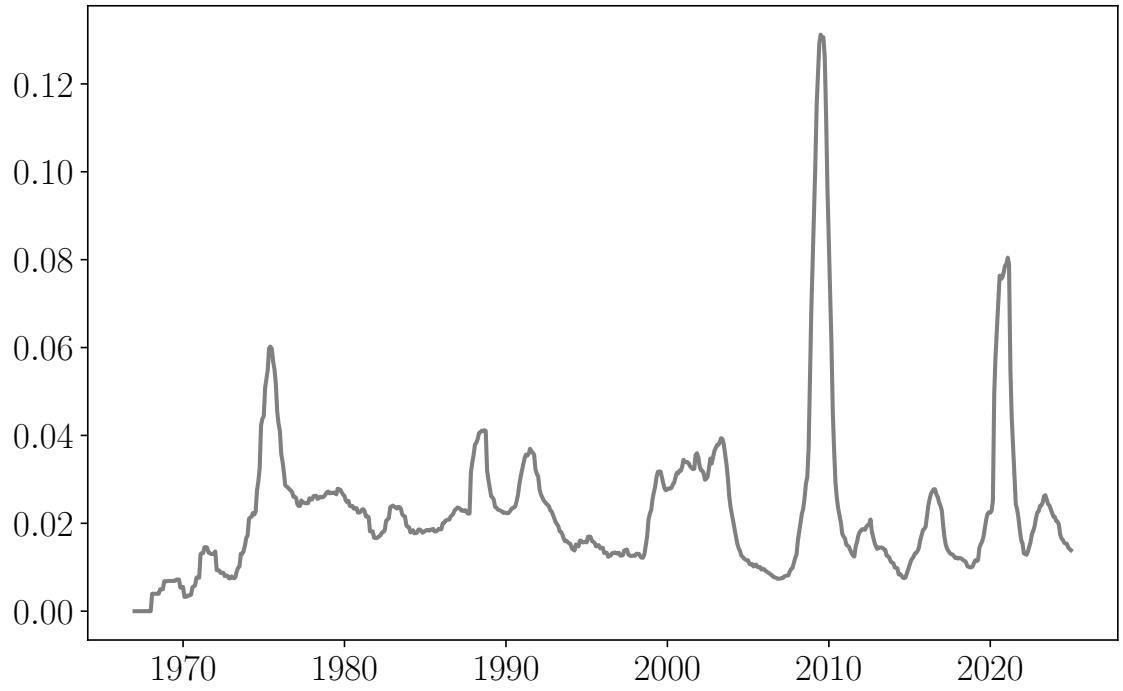

Figure 4
Fraction of firms with equity-to-bond momentum spillover
The figure plots the monthly fraction of firms satisfying the equity-to-bond spillover condition in equation (19), evaluated using the estimated model-implied spillover covariance, $\widehat{\mathcal{S}}_t = \widehat{\mathrm{Cov}}_t(dg^D, r)$, from equation (18), over 1966–2024. The series is smoothed using a twelve-month moving average.

	All	$\text{Cov}_t < 0$	$\text{Cov}_t > 0$
$h = 1$	-0.006	-0.029	0.052
	(-0.50)	(-2.11)	(2.24)
$h = 2$	0.016	0.003	0.050
	(1.35)	(0.24)	(1.99)
$h = 3$	0.048	0.027	0.099
	(3.89)	(1.92)	(4.09)
$h = 6$	0.116	0.100	0.155
	(8.45)	(6.36)	(5.66)
$h = 12$	0.218	0.216	0.223
	(12.51)	(11.13)	(6.02)

Table 1
Simulation results: Time-series momentum
The table reports time-series momentum returns in simulated data. For each firm i, look-back horizon $h \in \{1, 2, 3, 6, 12\}$ months, and month t, we compute the strategy's return as $\text{sign}(\text{signal}_{i,t,h})\, r_{i,t+1}$, where $r_{i,t+1}$ is the next-month holding period return. The signal is the past realized h-month return minus the risk-free accrual over the same window. The column *All* pools all firms, while the columns $\text{Cov}_t < 0$ and $\text{Cov}_t > 0$ report results for firms that fail and satisfy, respectively, the equity time-series momentum condition in equation (9), evaluated using the model-implied covariance $\text{Cov}_t(dg, r)$ in equation (12). Returns are expressed in percent per month.

	N	Mean	Median	Std	P5	P25	P75	P95
Panel A: All firms								
Leverage	1,885,076	0.263	0.211	0.232	0.000	0.060	0.417	0.714
Input Vol	1,885,076	0.333	0.258	0.303	0.078	0.165	0.409	0.819
Cov ($\times 10^3$)	1,885,021	-0.846	-0.082	4.711	-4.077	-0.399	-0.002	1.941
Cov AR(1)	9,769	0.417	0.465	0.337	-0.130	0.146	0.692	0.909
Panel B: $\widehat{\mathrm{Cov}}_t > 0$								
Leverage	225,306	0.431	0.437	0.220	0.060	0.262	0.605	0.775
Input Vol	225,306	0.637	0.500	0.522	0.203	0.339	0.755	1.511
Cov ($\times 10^3$)	225,306	1.835	1.426	1.608	0.027	0.372	3.084	4.824
Cov AR(1)	2,914	0.397	0.460	0.336	-0.159	0.130	0.671	0.857
Panel C: $\widehat{\mathrm{Cov}}_t < 0$								
Leverage	1,659,715	0.240	0.185	0.224	0.000	0.046	0.378	0.687
Input Vol	1,659,715	0.292	0.238	0.230	0.074	0.154	0.365	0.688
Cov ($\times 10^3$)	1,659,715	-1.209	-0.119	4.874	-4.776	-0.498	-0.019	-0.000
Cov AR(1)	6,855	0.426	0.468	0.337	-0.115	0.149	0.701	0.927

Table 2
Summary statistics
This table reports summary statistics for the firm-month panel over 1966–2024. Leverage is defined as the ratio of debt to total assets. Input Vol, $\sqrt{V}$, is the estimated input volatility obtained from the iterative procedure described in Section 4.1. Cov is the firm-level model-implied covariance, $\widehat{\mathrm{Cov}}_t(dg, r)$, estimated based on equation (12) and used to evaluate the equity time-series momentum condition in equation (9). Cov AR(1) is the firm-level monthly autocorrelation of $\widehat{\mathrm{Cov}}_t(dg, r)$. Panel A pools all firm-month observations, while Panels B and C condition on the sign of $\widehat{\mathrm{Cov}}_t(dg, r)$ in each month. For the Cov AR(1) measure, firms are assigned to Panel B or C according to the sign of their mean covariance. For each variable, we report the number of observations, mean, median, standard deviation, and the 5th, 25th, 75th, and 95th percentiles.

	All	$\widehat{\mathrm{Cov}}_t < 0$	$\widehat{\mathrm{Cov}}_t > 0$	Diff
$h = 1$	-0.289	-0.284	0.041	0.302
	(-3.20)	(-3.16)	(0.21)	(1.64)
$h = 2$	-0.347	-0.343	0.153	0.430
	(-3.36)	(-3.36)	(0.71)	(2.15)
$h = 3$	-0.144	-0.139	0.330	0.487
	(-1.39)	(-1.36)	(1.45)	(2.49)
$h = 6$	-0.020	-0.028	0.811	0.841
	(-0.16)	(-0.24)	(3.14)	(3.83)
$h = 12$	0.307	0.303	0.741	0.445
	(2.67)	(2.73)	(2.86)	(1.94)

Table 3
Time-series momentum in U.S. equities
The table reports value-weighted long-short time-series momentum returns. For each lookback horizon $h \in \{1, 2, 3, 6, 12\}$ months and month t, firms are sorted into a winner portfolio, consisting of firms with a positive past h-month return in excess of the risk-free rate, and a loser portfolio, consisting of firms with a negative past excess return. Firm-months are classified at the formation date t according to the equity time-series momentum condition in equation (9), evaluated using the model-implied $\widehat{\mathrm{Cov}}_t(dg, r)$ from equation (12). Within each covariance group, the time-series momentum return in month $t+1$ is the value-weighted return of winners minus the value-weighted return of losers, where weights are based on lagged equity market value. The column *All* pools all firms, while the columns $\widehat{\mathrm{Cov}}_t < 0$ and $\widehat{\mathrm{Cov}}_t > 0$ report results for firms with negative and positive model-implied covariance, respectively. *Diff* is the difference between the $\widehat{\mathrm{Cov}}_t > 0$ and $\widehat{\mathrm{Cov}}_t < 0$ portfolio returns, formed each month when both portfolios are available. Reported means are time-series averages of monthly portfolio returns, expressed in percent per month. t-statistics in parentheses are based on Newey–West standard errors with five lags.

	All	$\widehat{\mathrm{Cov}}_t < 0$	$\widehat{\mathrm{Cov}}_t > 0$	Diff
		Panel A: FF3 alphas		
$h = 1$	-0.292	-0.272	0.060	0.305
	(-3.06)	(-2.83)	(0.31)	(1.65)
$h = 2$	-0.351	-0.342	0.177	0.440
	(-3.29)	(-3.21)	(0.81)	(2.15)
$h = 3$	-0.140	-0.119	0.365	0.498
	(-1.29)	(-1.10)	(1.55)	(2.45)
$h = 6$	0.002	-0.008	0.823	0.834
	(0.01)	(-0.07)	(3.13)	(3.66)
$h = 12$	0.328	0.336	0.750	0.423
	(2.87)	(3.02)	(2.82)	(1.80)
		Panel B: FF5 alphas		
$h = 1$	-0.380	-0.352	-0.057	0.268
	(-3.74)	(-3.48)	(-0.28)	(1.44)
$h = 2$	-0.435	-0.415	0.011	0.348
	(-3.85)	(-3.70)	(0.05)	(1.73)
$h = 3$	-0.179	-0.150	0.224	0.397
	(-1.58)	(-1.33)	(0.96)	(1.96)
$h = 6$	0.004	-0.006	0.734	0.749
	(0.03)	(-0.05)	(2.75)	(3.23)
$h = 12$	0.315	0.325	0.720	0.403
	(2.70)	(2.87)	(2.76)	(1.74)

Table 4
Time-series momentum in U.S. equities: Risk-adjusted returns
The table reports FF3- and FF5-adjusted alphas of value-weighted long-short time-series momentum returns. For each lookback horizon $h \in \{1, 2, 3, 6, 12\}$ months and month t, firms are sorted into winner and loser portfolios as in Table 3, and the value-weighted winner-minus-loser return is formed in month $t + 1$. The reported alpha is the intercept from a time-series regression of this monthly return on the FF3 factors in Panel A or the FF5 factors in Panel B. Firm-months are classified at the formation date t according to the equity time-series momentum condition in equation (9), evaluated using the model-implied $\widehat{\mathrm{Cov}}_t(dg, r)$ from equation (12). The column *All* pools all firms, while the columns $\widehat{\mathrm{Cov}}_t < 0$ and $\widehat{\mathrm{Cov}}_t > 0$ report results for firms with negative and positive model-implied covariance, respectively. *Diff* is the alpha of the monthly difference between the $\widehat{\mathrm{Cov}}_t > 0$ and $\widehat{\mathrm{Cov}}_t < 0$ portfolio returns. Alphas are expressed in percent per month. t-statistics in parentheses are based on Newey–West standard errors with five lags.

	All	$\widehat{\mathrm{Cov}}_t < 0$	$\widehat{\mathrm{Cov}}_t > 0$	Diff
Panel A: Holding horizon of 3 months				
$h = 1$	-0.442	-0.398	0.067	0.403
	(-2.46)	(-2.26)	(0.18)	(1.27)
$h = 2$	-0.439	-0.384	0.563	0.878
	(-1.91)	(-1.73)	(1.25)	(2.20)
$h = 3$	-0.225	-0.189	0.973	1.176
	(-0.90)	(-0.79)	(1.92)	(2.97)
$h = 6$	0.128	0.069	1.925	1.828
	(0.44)	(0.25)	(3.25)	(3.79)
$h = 12$	0.923	0.917	2.091	1.216
	(2.87)	(2.98)	(3.51)	(2.64)
Panel B: Holding horizon of 6 months				
$h = 1$	-0.299	-0.272	0.881	1.002
	(-1.04)	(-1.00)	(1.47)	(1.91)
$h = 2$	-0.134	-0.088	1.869	1.869
	(-0.38)	(-0.25)	(2.53)	(3.03)
$h = 3$	0.214	0.216	2.525	2.257
	(0.52)	(0.56)	(3.03)	(3.60)
$h = 6$	1.042	1.037	3.846	2.919
	(2.31)	(2.43)	(4.35)	(4.20)
$h = 12$	1.769	1.757	3.395	1.674
	(3.08)	(3.14)	(3.46)	(2.23)

Table 5
Time-series momentum in U.S. equities: Alternative holding horizons
The table reports value-weighted long-short time-series momentum returns for two longer holding-period horizons. For each lookback horizon $h \in \{1, 2, 3, 6, 12\}$ months and month t, firms are sorted into winner and loser portfolios. Panel A uses a three-month holding period, while Panel B uses a six-month holding period. Firm-months are classified at the formation date t according to the equity time-series momentum condition in equation (9), evaluated using the model-implied $\widehat{\mathrm{Cov}}_t(dg, r)$ from equation (12). Within each covariance group, the time-series momentum return is the value-weighted return of winners minus the value-weighted return of losers, with weights based on lagged equity market value, accumulated over the holding horizon. The column *All* pools all firms, while the columns $\widehat{\mathrm{Cov}}_t < 0$ and $\widehat{\mathrm{Cov}}_t > 0$ report results for firms with negative and positive model-implied covariance, respectively. *Diff* is the difference between the $\widehat{\mathrm{Cov}}_t > 0$ and $\widehat{\mathrm{Cov}}_t < 0$ portfolio returns, formed each month when both portfolios are available. Reported means are time-series averages of cumulative portfolio returns, expressed in percent. t-statistics in parentheses are based on Newey–West standard errors with five lags.

	All	$\widehat{\mathrm{Cov}}_t < 0$	$\widehat{\mathrm{Cov}}_t > 0$	Diff
$h = 1$	-0.456	-0.456	–	–
	(-3.43)	(-3.43)		
$h = 2$	-0.329	-0.329	–	–
	(-2.30)	(-2.30)		
$h = 3$	-0.312	-0.312	–	–
	(-2.31)	(-2.31)		
$h = 6$	0.039	0.039	–	–
	(0.26)	(0.26)		
$h = 12$	0.276	0.276	–	–
	(1.71)	(1.71)		

Table 6
Time-series momentum in U.S. equities: Low-leverage, low-volatility firms
The table repeats the baseline value-weighted long-short time-series momentum test from Table 3, restricting the sample to firms with leverage, defined as debt to assets, below 5% and estimated input volatility $\sqrt{V}$ below 50%. These restrictions place the subsample deep within the reversal region shown in Figure 1. Firm-months are classified at the formation date t according to the equity time-series momentum condition in equation (9), evaluated using the model-implied $\widehat{\mathrm{Cov}}_t(dg, r)$ from equation (12). The column *All* pools all firms, while the columns $\widehat{\mathrm{Cov}}_t < 0$ and $\widehat{\mathrm{Cov}}_t > 0$ report results for firms with negative and positive model-implied covariance, respectively. *Diff* is the difference between the $\widehat{\mathrm{Cov}}_t > 0$ and $\widehat{\mathrm{Cov}}_t < 0$ portfolio returns. Reported means are time-series averages of monthly portfolio returns, expressed in percent per month. t-statistics in parentheses are based on Newey–West standard errors with five lags.

	Double-sort W−L	Cov Diff
$h = 1$	-0.203	0.148
	(-1.74)	(0.74)
$h = 2$	-0.173	0.365
	(-1.30)	(1.86)
$h = 3$	0.126	0.270
	(0.92)	(1.28)
$h = 6$	0.150	0.913
	(1.08)	(4.25)
$h = 12$	0.565	0.477
	(3.62)	(2.04)

Table 7
Time-series momentum within leverage × volatility portfolios
The table reports value-weighted firm-level time-series momentum returns within portfolios formed from an independent 2×3 sort on leverage and input volatility, $\sqrt{V}$. Each month, firms are assigned to leverage and input-volatility portfolios. Within each portfolio, a firm is held long if its past h-month return exceeds the risk-free accrual over the same period and short otherwise. Firm-level contributions are weighted by lagged equity market value. The column *Double-sort W−L* reports the portfolio's winner-minus-loser return. The column *Cov Diff* is the within-portfolio difference between the winner-minus-loser returns of firms satisfying and failing the equity time-series momentum condition in equation (9), evaluated using the model-implied $\widehat{\mathrm{Cov}}_t(dg, r)$ from equation (12). In a given month, a portfolio qualifies only if each covariance group contains at least five firms, and it enters the pooled sample only if it qualifies in at least five months. Returns are averaged across qualifying portfolios, with each portfolio weighted by the number of firms in its smaller covariance group. Reported means are time-series averages of the monthly pooled returns, expressed in percent per month. t-statistics in parentheses are based on Newey–West standard errors with five lags.

	(1)	(2)	(3)	(4)	(5)
Intercept	1.824	1.817	1.866	1.851	1.866
	(2.75)	(2.73)	(2.78)	(2.80)	(2.80)
Past return	0.001	0.003	0.000	0.003	0.007
	(0.79)	(1.50)	(0.18)	(2.12)	(2.76)
Cov > 0	-0.408	-0.390	-0.383	-0.413	-0.399
	(-3.27)	(-3.10)	(-2.75)	(-3.25)	(-2.80)
Past return $\times$Cov > 0	0.009	0.008	0.008	0.008	0.007
	(3.04)	(2.84)	(3.04)	(2.97)	(2.74)
log-Leverage	0.086	0.075	0.081	0.085	0.061
	(1.08)	(0.82)	(1.01)	(1.05)	(0.68)
Input Vol $\sqrt{V}$	-0.683	-0.704	-0.701	-0.681	-0.742
	(-3.77)	(-3.94)	(-3.10)	(-3.81)	(-3.26)
Credit rating	-0.013	-0.013	-0.013	-0.007	-0.006
	(-1.75)	(-1.75)	(-1.73)	(-1.82)	(-1.47)
Past return $\times$ log-Leverage		0.002			0.005
		(1.54)			(2.50)
Past return $\times$ Input Vol			0.004		0.004
			(1.11)		(0.95)
Past return $\times$ Credit rating				0.000	0.000
				(0.48)	(0.31)
Controls	Y	Y	Y	Y	Y
Industry dummies	Y	Y	Y	Y	Y
Average R^2	0.290	0.293	0.293	0.293	0.299

Table 8
Fama-MacBeth regressions: Momentum and the equity momentum condition
The table reports time-series averages of the monthly cross-sectional regression coefficients obtained from estimating equation (21). The dependent variable is the firm's return in month $t+1$. The key regressors are the past 12-month excess return, $r^e_{i,t-12:t}$, an indicator for whether the firm satisfies the equity time-series momentum condition in equation (9), evaluated using the model-implied $\widehat{\mathrm{Cov}}_{it}(dg, r)$ from equation (12), log leverage, input volatility $\sqrt{V}$, credit rating, and their interactions. Controls include log market equity, log book-to-market, gross profits to assets, log analyst coverage, log turnover, and industry dummies. Coefficients are expressed in percent per month. t-statistics in parentheses are based on Newey–West standard errors. Average R^2 is the time-series mean of the monthly cross-sectional R^2.

	All	$\widehat{\text{Cov}}_t < 0$	$\widehat{\text{Cov}}_t > 0$	Diff
$h = 1$	-0.283	-0.282	–	–
	(-3.78)	(-3.77)		
$h = 2$	-0.256	-0.255	–	–
	(-3.27)	(-3.26)		
$h = 3$	-0.300	-0.300	–	–
	(-3.04)	(-3.04)		
$h = 6$	-0.404	-0.403	–	–
	(-2.15)	(-2.14)		
$h = 12$	-0.205	-0.207	–	–
	(-2.34)	(-2.35)		

Table 9
Time-series momentum in corporate bonds
The table reports firm-level time-series momentum returns for corporate bonds sorted on their own past returns. CRSP common stocks are matched to their bonds in TRACE over 2002–2024. For each lookback horizon $h \in \{1, 2, 3, 6, 12\}$ months and month t, a firm's bond position is long if its past h-month Treasury-adjusted excess return is positive and short otherwise, with the holding-period return measured in month $t+1$. Firm-months are classified at the formation date t according to the bond time-series momentum condition in equation (15), evaluated using the model-implied $\widehat{\text{Cov}}_t(dg^D, r^D)$ from equation (16). Within each month, firm-level contributions are averaged using weights based on the firm's lagged market value of outstanding bonds. The column *All* pools all firms, while the columns $\widehat{\text{Cov}}_t < 0$ and $\widehat{\text{Cov}}_t > 0$ report results for firms with negative and positive model-implied covariance, respectively. *Diff* is the difference between the $\widehat{\text{Cov}}_t > 0$ and $\widehat{\text{Cov}}_t < 0$ columns. Reported means are time-series averages of monthly portfolio returns, expressed in percent per month. t-statistics in parentheses are based on Newey–West standard errors with five lags.

	All	$\widehat{\mathcal{S}}_t < 0$	$\widehat{\mathcal{S}}_t > 0$	Diff
$h = 1$	0.177	0.145	1.048	0.869
	(3.48)	(4.83)	(2.39)	(2.01)
$h = 2$	0.183	0.165	0.987	0.767
	(3.44)	(3.82)	(2.39)	(1.88)
$h = 3$	0.143	0.127	0.650	0.471
	(3.41)	(4.38)	(1.87)	(1.34)
$h = 6$	0.064	0.093	0.377	0.271
	(1.65)	(3.21)	(0.94)	(0.68)
$h = 12$	0.072	0.073	0.177	0.110
	(1.51)	(1.91)	(0.36)	(0.23)

Table 10
Equity-to-bond momentum spillover
The table reports firm-level corporate bond returns using past equity returns as the signal. CRSP common stocks are matched to their bonds in TRACE over 2002–2024. For each firm i, lookback horizon $h \in \{1, 2, 3, 6, 12\}$ months, and month t, the bond position in month $t+1$ takes the sign of the firm's past h-month equity excess return, and the realized return is the next-month Treasury-adjusted bond excess return. Firm-months are classified at the formation date t according to the equity-to-bond spillover condition in equation (19), evaluated using the model-implied spillover covariance $\widehat{\mathcal{S}}_t = \widehat{\mathrm{Cov}}_t(dg^D, r)$ from equation (18). Within each month and group, firm-level contributions are averaged using weights based on the firm's lagged market value of outstanding bonds. The column *All* pools all firms, while the columns $\widehat{\mathcal{S}}_t < 0$ and $\widehat{\mathcal{S}}_t > 0$ report results for firms with negative and positive spillover covariance, respectively. *Diff* is the difference between the $\widehat{\mathcal{S}}_t > 0$ and $\widehat{\mathcal{S}}_t < 0$ portfolio returns, formed each month when both portfolios are available. Reported means are expressed in percent per month. t-statistics in parentheses are based on Newey–West standard errors with five lags.

		$\widehat{\mathcal{S}}_t < 0$	$\widehat{\mathcal{S}}_t > 0$	Diff
	Liquid	0.179	1.091	0.872
		(5.12)	(2.22)	(1.79)
$h = 1$	Mid	0.126	2.217	1.895
		(3.75)	(2.40)	(2.08)
	Illiquid	0.102	2.458	2.228
		(2.84)	(1.74)	(1.68)
	Liquid	0.196	1.399	1.096
		(3.75)	(2.67)	(2.14)
$h = 2$	Mid	0.152	1.514	1.147
		(4.62)	(1.50)	(1.14)
	Illiquid	0.095	1.720	1.576
		(3.17)	(1.54)	(1.44)
	Liquid	0.148	0.641	0.437
		(4.62)	(1.68)	(1.14)
$h = 3$	Mid	0.131	1.513	1.265
		(3.79)	(1.75)	(1.43)
	Illiquid	0.107	1.740	1.636
		(3.38)	(1.62)	(1.55)
	Liquid	0.114	0.653	0.569
		(3.37)	(1.43)	(1.21)
$h = 6$	Mid	0.093	0.307	0.093
		(2.50)	(0.22)	(0.07)
	Illiquid	0.057	4.616	4.255
		(1.54)	(1.63)	(1.54)
	Liquid	0.102	-0.031	-0.145
		(2.24)	(-0.07)	(-0.31)
$h = 12$	Mid	0.073	-1.672	-1.795
		(1.21)	(-1.89)	(-2.02)
	Illiquid	0.021	-0.027	0.033
		(0.60)	(-0.02)	(0.02)

Table 11
Equity-to-bond momentum spillover across bond liquidity groups
The table reports the equity-to-bond momentum spillover from Table 10, separately across bond liquidity groups. Each month, firm-month observations are assigned to liquidity terciles based on the firm-level average of two lagged liquidity proxies: the Amihud illiquidity measure and the fraction of zero-trading days. *Liquid* denotes the most liquid tercile, while *Illiquid* denotes the least liquid tercile. The columns $\widehat{\mathcal{S}}_t < 0$ and $\widehat{\mathcal{S}}_t > 0$ report results for firms that fail and satisfy the equity-to-bond spillover condition in equation (19), respectively, evaluated using the model-implied spillover covariance $\widehat{\mathcal{S}}_t = \widehat{\mathrm{Cov}}_t(dg^D, r)$ from equation (18). *Diff* is the difference between the $\widehat{\mathcal{S}}_t > 0$ and $\widehat{\mathcal{S}}_t < 0$ portfolio returns, formed each month when both portfolios are available. Reported means are expressed in percent per month. t-statistics in parentheses are based on Newey–West standard errors with five lags.

	All	$\widehat{\mathcal{S}}_t < 0$	$\widehat{\mathcal{S}}_t > 0$	Diff
Panel A: Short-term bonds				
$h = 1$	0.089	0.055	0.929	0.874
	(2.23)	(4.62)	(2.12)	(2.04)
$h = 2$	0.065	0.061	0.729	0.637
	(2.19)	(3.01)	(1.60)	(1.42)
Panel B: Medium-term bonds				
$h = 1$	0.216	0.197	1.308	1.050
	(3.50)	(4.10)	(2.62)	(2.05)
$h = 2$	0.240	0.212	1.365	1.058
	(3.21)	(3.46)	(3.33)	(2.43)
Panel C: Long-term bonds				
$h = 1$	0.275	0.228	1.423	1.096
	(2.90)	(3.53)	(1.92)	(1.45)
$h = 2$	0.282	0.226	1.067	0.719
	(3.06)	(3.85)	(2.17)	(1.45)

Table 12
Equity-to-bond spillover by bond maturity
The table reports the equity-to-bond momentum spillover from Table 10, separately for short- (≤ 5 years), medium- (5–10 years), and long-maturity (> 10 years) bonds, classified by time to maturity. The column *All* pools all firms, while the columns $\widehat{\mathcal{S}}_t < 0$ and $\widehat{\mathcal{S}}_t > 0$ report results for firms that fail and satisfy the equity-to-bond spillover condition in equation (19), respectively, evaluated using the model-implied spillover covariance $\widehat{\mathcal{S}}_t = \widehat{\mathrm{Cov}}_t(dg^D, r)$ from equation (18). *Diff* is the difference between the $\widehat{\mathcal{S}}_t > 0$ and $\widehat{\mathcal{S}}_t < 0$ portfolio returns, formed each month when both portfolios are available. Reported means are expressed in percent per month. t-statistics in parentheses are based on Newey–West standard errors with five lags.

	All	$\widehat{\mathcal{S}}_t < 0$	$\widehat{\mathcal{S}}_t > 0$	Diff
Panel A: Speculative Grade				
$h = 1$	0.489	0.363	1.433	0.980
	(4.14)	(7.31)	(2.90)	(2.29)
$h = 2$	0.380	0.333	1.316	0.903
	(3.44)	(3.72)	(2.93)	(2.16)
Panel B: Lower Investment Grade				
$h = 1$	0.148	0.153	0.419	0.266
	(5.30)	(5.76)	(1.03)	(0.63)
$h = 2$	0.203	0.213	-0.218	-0.707
	(4.53)	(4.22)	(-0.55)	(-1.61)
Panel C: Higher Investment Grade				
$h = 1$	0.084	0.086	-0.497	-0.750
	(1.57)	(1.91)	(-0.98)	(-1.70)
$h = 2$	0.104	0.083	0.353	-0.006
	(1.76)	(1.77)	(0.94)	(-0.02)

Table 13
Equity-to-bond spillover by credit rating
The table reports the equity-to-bond momentum spillover from Table 10, separately for speculative-grade, lower investment-grade, and higher investment-grade bonds. The column *All* pools all firms, while the columns $\widehat{\mathcal{S}}_t < 0$ and $\widehat{\mathcal{S}}_t > 0$ report results for firms that fail and satisfy the equity-to-bond spillover condition in equation (19), respectively, evaluated using the model-implied spillover covariance $\widehat{\mathcal{S}}_t = \widehat{\mathrm{Cov}}_t(dg^D, r)$ from equation (18). *Diff* is the difference between the $\widehat{\mathcal{S}}_t > 0$ and $\widehat{\mathcal{S}}_t < 0$ portfolio returns, formed each month when both portfolios are available. Reported means are expressed in percent per month. t-statistics in parentheses are based on Newey–West standard errors with five lags.

	Median	P_{75}	P_{90}	P_{98}	Max
	Panel A: Increase in Losers' Asset Elasticity				
$\eta^A_{\mathcal{L}}$	1.500	1.750	1.930	2.250	2.500
$P(r^M_{t+1} < -11\%)$	0%	0.025%	0.383%	3.381%	7.258%
	Panel B: Increase in Winners' Asset Elasticity				
$\eta^A_{\mathcal{W}}$	1.250	1.350	1.450	1.650	2.090
$P(r^M_{t+1} < -11\%)$	0%	0%	0%	0%	0.045%
	Panel C: Increase in Losers' Variance Elasticity				
$\eta^V_{\mathcal{L}}$	0.025	0.034	0.063	0.119	0.240
$P(r^M_{t+1} < -11\%)$	0%	0%	0%	0%	0.395%
	Panel D: Increase in Winners' Variance Elasticity				
$\eta^V_{\mathcal{W}}$	0.015	0.040	0.080	0.140	0.200
$P(r^M_{t+1} < -11\%)$	0%	0%	0%	0.272%	3.432%

Table 14
Momentum crashes simulation
The table reports the probability of a momentum crash at different levels of the asset and variance elasticities, η^A and η^V, where a crash is defined as a next-month return below -11%. In each panel, one elasticity varies across its empirical distribution while the other three are fixed at their empirical medians: $\eta^A_{\mathcal{L}} = 1.500$, $\eta^A_{\mathcal{W}} = 1.250$, $\eta^V_{\mathcal{L}} = 0.025$, and $\eta^V_{\mathcal{W}} = 0.015$. The probabilities are based on 100,000 simulated shocks. We set $\mu - r_f = 4\%$, $\lambda_V = -1.75$, $\rho^{\text{agg}} = -0.15$, $\sigma_A = 20\%$, and $\sigma_V = 80\%$ for both winners and losers.

	Panel A: Momentum crash predictors			
	(1)	**(2)**	**(3)**	**(4)**
Expected mom. return μ^M	11.382			
	(2.15)			
Fraction ω_t with Cov >0		3.088		
		(2.17)		
Asset shock asymmetry Δ^A			-14.355	
			(-2.66)	
Variance shock asymmetry Δ^V				-29.093
				(-4.32)
Market return $R^{mkt}_{t-24:t}$	-0.470	-0.658	-0.888	-0.016
	(-0.56)	(-0.75)	(-0.95)	(-0.02)
Market volatility $Vol^{mkt}_{t-6:t}$	12.691	10.166	13.400	4.435
	(1.65)	(1.27)	(1.89)	(0.53)
Pseudo-R^2	0.055	0.052	0.070	0.095

	Panel B: Momentum crash predictors' decomposition					
	(1)	**(2)**	**(3)**	**(4)**	**(5)**	**(6)**
Assets: $\eta^A_{\mathcal{W}} - \eta^A_{\mathcal{L}}$	-1.74					
	(-3.37)					
Variance: $\eta^V_{\mathcal{W}} - \eta^V_{\mathcal{L}}$		-27.96				
		(-5.23)				
Losers asset loading $\Delta^A_{\mathcal{L}}$			16.49			
			(3.24)			
Winners asset loading $\Delta^A_{\mathcal{W}}$				-10.23		
				(-0.86)		
Losers variance loading $\Delta^V_{\mathcal{L}}$					28.03	
					(6.00)	
Winners variance loading $\Delta^V_{\mathcal{W}}$						16.42
						(1.33)
Pseudo-R^2	0.050	0.075	0.041	0.004	0.094	0.004

Table 15
Momentum crashes in U.S. equities
The table reports predictive regressions for momentum crashes in the CRSP sample of common stocks over 1966–2024. The dependent variable equals one when the winner-minus-loser return falls below the 5th percentile of its distribution, corresponding to a return below −11%, and zero otherwise. Panel A includes the expected momentum return, μ^M, the fraction of firms satisfying the equity time-series momentum condition in equation (9), ω_t, and the momentum return loadings on asset and variance shocks, Δ^A and Δ^V. Controls are the past 24-month market return $R^{\text{mkt}}_{t-24:t}$ and trailing 6-month market volatility $Vol^{\text{mkt}}_{t-6:t}$. Panel B decomposes the asset- and variance-shock predictors into winner- and loser-leg components. The table reports coefficient estimates, with t-statistics based on robust standard errors in parentheses.

Internet Appendix

Panel A: Momentum Condition

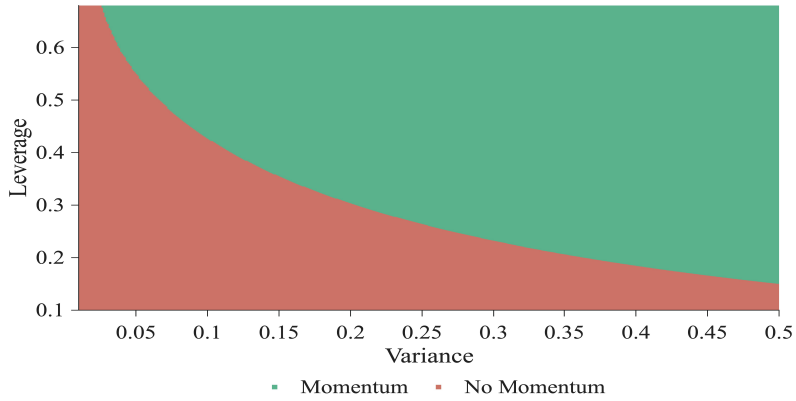

Panel B: Overlap

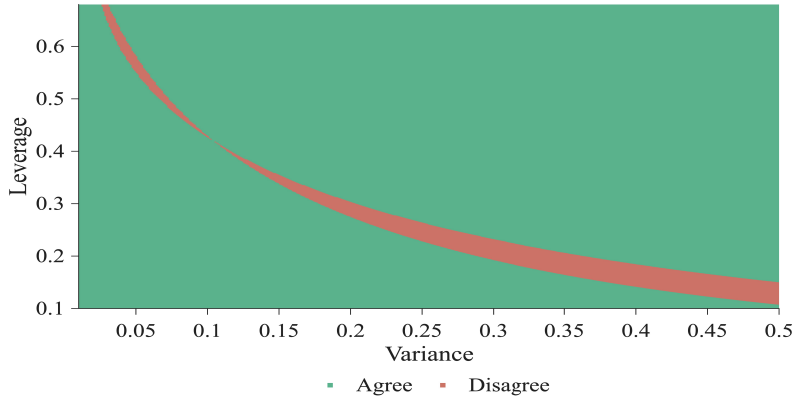

Figure IA.1
Equity momentum condition in the stochastic-variance model
The figure plots the sign of $\mathrm{Cov}_t^{SV}(dg, r)$ implied by equation (13) in Panel A and its overlap with the sign of $\mathrm{Cov}_t(dg, r)$ in equation (12) in Panel B, as functions of leverage, F/A, and variance, V. In Panel A, the green region identifies states for which $\mathrm{Cov}_t^{SV}(dg, r) > 0$, implying momentum, while the red region identifies states for which $\mathrm{Cov}_t^{SV}(dg, r) < 0$, implying reversal. In Panel B, the green and red regions indicate agreement and disagreement, respectively, between the two conditions. The annualized parameters are: asset risk premium $\mu - r_f = 4\%$, variance-risk price $\lambda_V = -1.75$, volatility of the variance process $\sigma_V = 0.40$, time to maturity $\tau = 1$, correlation between asset and variance shocks $\rho = -0.15$, mean-reversion speed $\kappa = 2.5$, and long-run variance level $\theta = 0.07$.

Panel A: Price of Asset Risk				
$\mu - r_f$	0.02	0.06	0.08	0.1
	0.827	0.962	1.045	1.146
	(4.13)	(3.80)	(3.82)	(3.94)
Panel B: Price of Variance Risk				
λ_V	-0.5	-1	-2	-3
	0.907	0.962	0.945	0.827
	(2.89)	(3.80)	(4.53)	(4.13)
Panel C: Correlation				
ρ	-0.05	-0.3	-0.6	-0.8
	0.884	0.819	0.808	0.780
	(3.36)	(3.98)	(4.42)	(4.43)
Panel D: Asset Volatility				
σ_A	0.05	0.15	0.25	0.4
	0.574	0.898	0.905	0.870
	(2.21)	(3.90)	(3.82)	(3.54)
Panel E: Variance Volatility				
σ_V	0.1	0.2	0.6	0.8
	0.870	0.899	0.754	0.574
	(3.54)	(3.84)	(3.30)	(2.21)
Panel F: Debt Maturity				
τ	0.5	2	3	4
	0.676	0.663	0.380	0.270
	(2.07)	(4.54)	(3.06)	(2.29)

Table IA.1
Time-series momentum in U.S. equities: Parameter sensitivity
The table reports *Diff*, the difference in value-weighted long-short time-series momentum returns between firms satisfying and failing the equity time-series momentum condition in equation (9), evaluated using the model-implied $\widehat{\mathrm{Cov}}_t(dg, r)$ from equation (12), for the six-month lookback horizon, $h = 6$, under alternative parameter choices. We vary one parameter at a time while holding all others at their baseline values. Reported means are time-series averages of monthly portfolio returns, expressed in percent per month. t-statistics in parentheses are based on Newey–West standard errors with five lags.

	All	$\widehat{\mathcal{S}}_t < 0$	$\widehat{\mathcal{S}}_t > 0$	Diff
$h = 1$	0.179	0.149	1.119	0.919
	(3.36)	(4.27)	(2.64)	(2.19)
$h = 2$	0.190	0.167	1.069	0.853
	(3.70)	(4.14)	(2.62)	(2.13)
$h = 3$	0.163	0.141	0.639	0.476
	(4.19)	(4.95)	(1.84)	(1.37)
$h = 6$	0.078	0.098	0.412	0.298
	(1.94)	(3.37)	(1.02)	(0.75)
$h = 12$	0.098	0.088	0.163	0.076
	(1.79)	(2.03)	(0.32)	(0.15)

Table IA.2
Robustness: Equity-to-bond spillover with accrued interest
The table repeats the equity-to-bond momentum spillover test from Table 10 using bond returns that include accrued interest. Firm-months are classified at the formation date t according to the equity-to-bond spillover condition in equation (19), evaluated using the model-implied spillover covariance $\widehat{\mathcal{S}}_t = \widehat{\mathrm{Cov}}_t(dg^D, r)$ from equation (18). The column *All* pools all firms, while the columns $\widehat{\mathcal{S}}_t < 0$ and $\widehat{\mathcal{S}}_t > 0$ report results for firms with negative and positive spillover covariance, respectively. *Diff* is the difference between the $\widehat{\mathcal{S}}_t > 0$ and $\widehat{\mathcal{S}}_t < 0$ portfolio returns, formed each month when both portfolios are available. Reported means are expressed in percent per month. t-statistics in parentheses are based on Newey–West standard errors with five lags.